

# Haptic feedback on the steering wheel near the vehicle's handling limits using wheel load sensing

J.J. van Doornik

Master of Science Thesis





# **Haptic feedback on the steering wheel near the vehicle's handling limits using wheel load sensing**

MASTER OF SCIENCE THESIS

For the degree of Master of Science in Mechanical Engineering at Delft  
University of Technology

J.J. van Doornik

June 23, 2014

Faculty of Mechanical, Maritime and Materials Engineering (3mE) · Delft University of  
Technology



The work in this thesis was supported by SKF and Prodrive.



Copyright © Delft Center for Systems and Control (DCSC)  
All rights reserved.





DELFT UNIVERSITY OF TECHNOLOGY  
DEPARTMENT OF  
DELFT CENTER FOR SYSTEMS AND CONTROL (DCSC)

The undersigned hereby certify that they have read and recommend to the Faculty of  
Mechanical, Maritime and Materials Engineering (3mE) for acceptance a thesis  
entitled

HAPTIC FEEDBACK ON THE STEERING WHEEL NEAR THE VEHICLE'S HANDLING  
LIMITS USING WHEEL LOAD SENSING

by

J.J. VAN DOORNIK

in partial fulfillment of the requirements for the degree of  
MASTER OF SCIENCE MECHANICAL ENGINEERING

Dated: June 23, 2014

Supervisor(s):

\_\_\_\_\_  
Prof.dr.ir. E.G.M. Holweg

\_\_\_\_\_  
Dr.ir. R. Happee

Reader(s):

\_\_\_\_\_  
Dr.ir. D.I. Katzourakis

\_\_\_\_\_  
Ir. B. Shyrokau

\_\_\_\_\_  
Ir. S.M.A.A. Kerst



---

# Abstract

Research in vehicle dynamics and vehicle control systems has increased a lot over the last decades due to the focus towards safety, driving comfort and emissions and the opportunities that come with the development of hybrid- and electric powertrains. Modern vehicles are equipped with many automated systems but automation can have disadvantages such as overreliance, complacency, nonvigilance, deskilling and confusing the driver. The goal of this thesis is to prevent loss of control by improving haptic feedback on the steering wheel near the vehicle's handling limits using wheel load sensing. Predicting when a vehicle starts to over- or understeer is a difficult task since it depends on the road surface and will only be revealed by vehicle states once it is already too late. The aligning moment of the tire drops before the lateral force actually saturates because of a decrease in pneumatic trail caused by tire contact patch deformation. This drop in aligning moment can be felt on the steering wheel and is an indication that a vehicle is close to the limit. However, the large ratio of mechanical to pneumatic trail and the increased power steering in modern vehicles makes the drop in aligning moment difficult to feel. If vehicles become steer-by-wire there is no feedback reaching the driver through the steering wheel at all.

The first part of this thesis consists of identification of the lateral force and aligning moment of the tires with Load Sensing Bearings (LSBs) from SKF. Estimating the lateral force has been done before and the results here show that estimation of the aligning moment is also possible. A Multiple Linear Regression Analysis (MLRA) is used to find first order linear models reconstructing the lateral force and aligning moment from measurements with the LSBs. Different models are derived based on measurements of strain gauges and hall effect sensors on the bearing. The second part of this thesis consists of experiments done at the Prodrive test track to investigate the improvement of haptic feedback using LSBs. The work is a follow-up study based on the Haptic Support Near the Limits (HSNL) system developed in a previous research project. The drop in aligning moment is measured with LSBs and amplified on the steering wheel. The results show that with this feedback drivers are indeed better capable of preventing saturation of the front tires but further research is needed on how the system can increase safety. The results show a decrease in control effort and workload with feedback which can increase driving pleasure and comfort for the driver.





---

# Table of Contents

<b>Acknowledgements</b>	<b>v</b>
<b>1 Introduction</b>	<b>1</b>
1-1 Background . . . . .	1
1-1-1 Different concepts . . . . .	1
1-1-2 Automation vs. manual control . . . . .	1
1-1-3 Steering . . . . .	2
1-2 Goal . . . . .	2
1-2-1 Vehicle dynamics . . . . .	3
1-2-2 Tires . . . . .	4
1-3 Content . . . . .	6
1-4 Hypothesis . . . . .	6
1-5 Stakeholders . . . . .	6
<b>2 Load sensing bearings</b>	<b>7</b>
2-1 Description . . . . .	7
2-1-1 Bearing . . . . .	7
2-1-2 Strain gauges . . . . .	8
2-1-3 Hall effect sensors . . . . .	8
2-1-4 BEaring Test SYstem (BETSY) . . . . .	9
2-2 Experiments . . . . .	9
2-2-1 Goal . . . . .	9
2-2-2 Instrumentation . . . . .	10
2-2-3 Calibration procedure . . . . .	11
2-3 Results . . . . .	13
2-3-1 Measurements . . . . .	13
2-3-2 Filtering . . . . .	18
2-3-3 System identification . . . . .	21
2-4 Conclusion . . . . .	29

<b>3 Haptic feedback</b>	<b>31</b>
3-1 Description . . . . .	31
3-1-1 General . . . . .	31
3-1-2 Model . . . . .	31
3-2 Experiments . . . . .	34
3-2-1 Goal . . . . .	34
3-2-2 Testing procedure . . . . .	34
3-2-3 Evaluation form . . . . .	35
3-3 Results . . . . .	36
3-3-1 Data processing . . . . .	36
3-3-2 Vehicle states . . . . .	37
3-3-3 Evaluation form . . . . .	41
3-4 Conclusion . . . . .	44
<b>Discussion</b>	<b>47</b>
<b>Conclusion</b>	<b>51</b>
<b>A Bearing information</b>	<b>53</b>
<b>B Wheatstone bridge</b>	<b>57</b>
<b>C Simulink model haptic controller</b>	<b>59</b>
<b>D Evaluation form</b>	<b>61</b>
<b>E Vehicle parameters</b>	<b>65</b>
<b>Bibliography</b>	<b>67</b>
<b>Glossary</b>	<b>69</b>
List of Acronyms . . . . .	69
List of Symbols . . . . .	70

---

# Acknowledgements

I would like to thank SKF and Prodrive for the opportunity to work on this project. A special thank you to professor Edward Holweg for making this possible. Many thanks to my supervisors: Dave Rollett (Prodrive) and Riender Happee (TU Delft). I want to thank Simon van Ballegooij and Henk Mol from SKF for their support with the LSBs, Diomidis Katzourakis for his support with the instrumentation in the Opel Astra and Stijn Kerst for his inputs concerning all instrumentation. Furthermore I want to thank the people at Prodrive and especially Adrian Hall and Duncan Macalister for their help in the workshop. Many thanks to the thirteen test subjects for taking part in the experiment.

Delft, University of Technology  
June 23, 2014

J.J. van Doornik





---

# Chapter 1

---

## Introduction

### 1-1 Background

Research in vehicle dynamics and vehicle control systems has increased a lot over the last decades due to the focus towards safety, driving comfort and emissions and the opportunities that come with the development of hybrid- and electric powertrains.

#### 1-1-1 Different concepts

Modern vehicles have to be equipped with basic Anti-lock Braking System (ABS) [1] and Electronic Stability Program (ESP) / Electronic Stability Control (ESC) systems [2][3] which help to improve stability and are developed for safety reasons. The introduction of Adaptive Cruise Control (ACC) improves driving comfort and emission reduction. Other intelligent vehicle control systems developed are Active Front Steering (AFS), Lane Departure Warning / Prevention (LDW/P), Obstacle Collision Avoidance System (OCAS), BLindspot Information System (BLIS) and more which are all part of the Advanced Driver Assistance Systems (ADAS). Recent luxury vehicles even come with systems like Intelligent Parking Assist System (IPAS) / Advanced Parking Guidance System (APGS) and Traffic Jam Assist(ant) (TJA) which are meant to increase driving comfort. These systems provide the first steps to fully autonomous driving. However, as [4] rightly concludes: "road safety will come through revolution in the automotive infrastructure rather than evolution on current safety systems".

#### 1-1-2 Automation vs. manual control

Reading the above one can question if autonomous driving is really desired. Driving can be a great pleasure and automation is not always more safe; general problems seen in automation include overreliance, complacency, nonvigilance, deskilling and confusing the driver [5]. A different option than full automation is the philosophy of haptic shared control. This means

providing augmented feedback on top of the intrinsic feedback that is already available to the driver. Haptic shared control keeps the driver in the loop and provides support when desired. This helps to prevent some of the general problems seen in automation and hopefully makes driving a fun experience again. Note that some problems seen in automation can still exist in the haptic shared control sense, and one has to be careful to draw conclusions on the improvement of safety by introducing a haptic shared control system [6]. Some systems may seem to improve safety but drivers actually tend to drive more dangerously and more on the limit which only causes more and more severe accidents. Difficulties in the haptic shared control domain are setting threshold values and deciding when to support the driver and when not. Supporting the driver in some tasks may increase driver satisfaction but might in fact decrease overall safety as stated above.

### 1-1-3 Steering

A basic steering wheel has two functions: transfer torque from driver to steering column and provide haptic feedback to the driver. The torque needed to rotate the steering wheel differs based on different factors such as vehicle velocity and tire forces. Rising demand for reductions in physical driver effort gave rise to the development of so called power assist steering systems. The first power assist systems were all based on hydraulics and are named Hydraulic Power Assisted Steering (HPAS). Disadvantages are that they are bulky, complex, inefficient and difficult to maintain. Later on most systems became Electric Power Assisted Steering (EPAS) which means the hydraulics are replaced with an electric actuator. The advantages of EPAS are that it is versatile, simple, efficient and inexpensive [7]. However, customers sometimes complain about the lack of steering feel of new cars equipped with an EPAS system. Currently most road vehicles still have a mechanical link between the steering wheel and the tires to make sure the system is reliable and fail-safe. In the future however at some point vehicles will become steer-by-wire and this will introduce new challenges for automotive engineers to provide the driver with accurate haptic feedback on the steering wheel.

## 1-2 Goal

In the literature study [8] prior to this thesis work a framework was established covering the theoretical aspects of driver haptics and wheel load sensing. The research question for this literature study was:

**How can we improve haptic feedback on the steering wheel near the vehicle's handling limits using wheel load sensing?**

The most important improvement is in terms of safety. More than 50 % of fatal accidents are annually the result of a single vehicle crash [9]. Haptic feedback on the steering wheel can help to reduce this number; the system acts near the vehicle's handling limits and should help the driver to prevent exceeding the limits thereby preventing loss of control. As described in Section 1-1-1 there are many successfully applied active safety systems such as AFS and ESP / ESC which automatically correct vehicle states if loss of control is likely [10][2].

So why would we use haptic feedback instead of an automated system?

This is where the next improvement can be achieved: in terms of driving pleasure and comfort. Providing more dynamic steering feel to the driver and keeping the driver in the loop can help to increase driving pleasure and make driving more comfortable since the driver feels when the handling limit is near. Increased driving pleasure can also help to prevent general problems seen in automation, such as: complacency, nonvigilance and deskilling [5]. A difficult issue however is that increased driving pleasure and comfort might also lead to more unsafe driving behavior compromising the improvements in terms of safety.

To understand how haptic feedback on the steering wheel can be improved using wheel load sensing, it is important to know the type of feedback that is normally available to drivers near the vehicle's handling limits.

### 1-2-1 Vehicle dynamics

So what do we want to achieve by improving haptic feedback to the driver? To answer that question we have to get a closer look at a steering vehicle. The radius of the corner a vehicle makes is determined by the steering angle and some other vehicle parameters [11] and of course if one drives more to the limits, the available grip of the road surface becomes important. This means that not every vehicle will respond exactly the same to the same steering angle and a vehicle can over- or understeer. Front-Wheel Drive (FWD) vehicles tend to be a bit understeered whilst Rear-Wheel Drive (RWD) vehicles are more likely to be slightly oversteered. In general a slightly understeered vehicle is preferred by most drivers because a vehicle in understeer is stable whereas in oversteer it is not. Our goal is to provide the driver with haptic feedback on the steering wheel as the limit is approaching and thereby hopefully prevent the driver from generating inputs leading to terminal understeer. Predicting when the vehicle starts to over- or understeer is a difficult task since it depends on the road surface and will only be revealed by vehicle states once it is too late. Tires however offer a mechanism to predict the limits before the vehicle starts to over- or understeer.

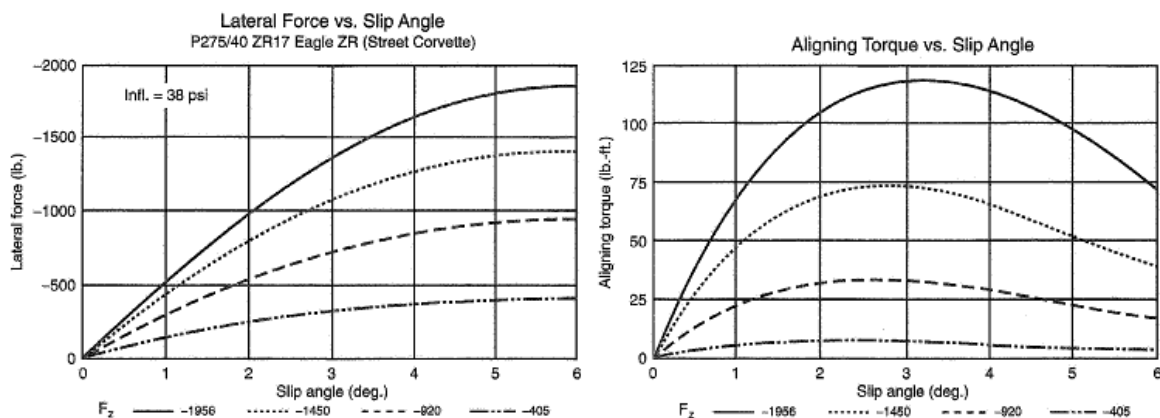
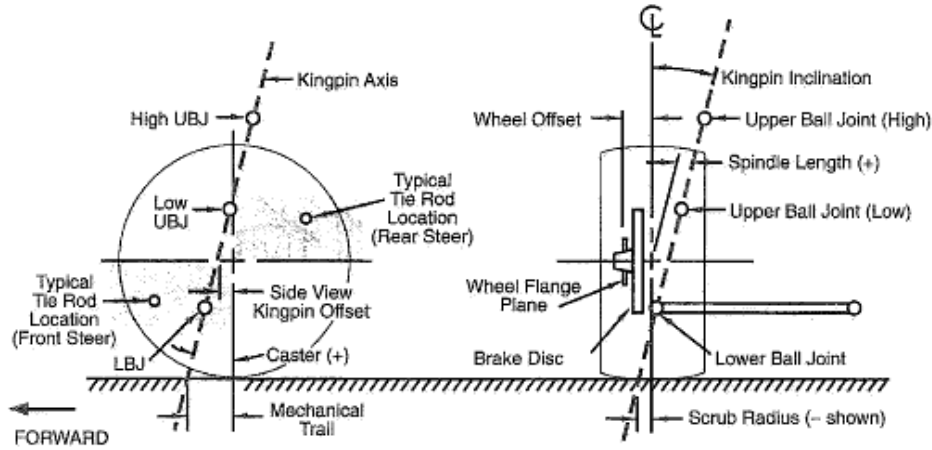


Figure 1-1: Lateral force and aligning moment vs. slip angle [11]

### 1-2-2 Tires

Apart from aerodynamic forces all external forces acting on a vehicle are generated at the four contact patches of the tire with the road. Each tire generates three forces and three moments. As a vehicle starts cornering the lateral force of the tires builds up. Due to lateral load transfer there is a shift of normal force from the inside to the outside tires. This means more lateral force will be generated by the outside tires. As can be seen in Figure 1-1 the lateral force saturates at higher slip angles depending on the road surface. Since there is no clear peak in the lateral force it is hard to measure when the limit is reached. However, the aligning moment of the tires has a clear peak before the lateral force saturates. The aligning moment is one of the most important contributors to the total steering torque the driver feels. The total steering torque is influenced by many other factors such as: toe, camber, caster, scrub radius, longitudinal force, vertical force, kingpin inclination angle, kingpin offset at the ground and more, see Figure 1-2.



**Figure 1-2:** Single tire parameters defining the mechanical trail ( $t_m$ ) [11]

If we neglect the smaller contributors and assume small longitudinal force (steady-state cornering), the aligning moment and steering torque can be calculated by:

$$M_z = (t_p) \cdot F_y$$

$$T_{steering} = (t_p + t_m) \cdot F_y \cdot \cos(\nu)$$

In this equation mechanical trail is fixed by the caster angle, wheel radius and kingpin offset of the vehicle which are all a result of the vehicles suspension design, see Figure 1-3. The key is the pneumatic trail which is variable and decreases with increasing lateral force due to deformation of the tire contact patch as can be seen in Figure 1-3 and Figure 1-4.



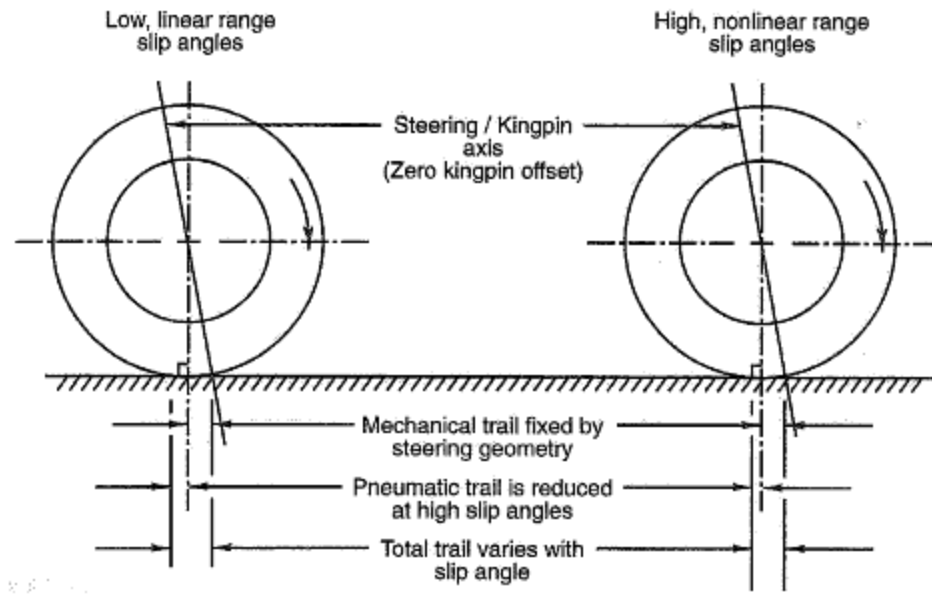


**Figure 1-3:** Mechanical trail ( $t_m$ ) and pneumatic trail ( $t_p$ ) [11]

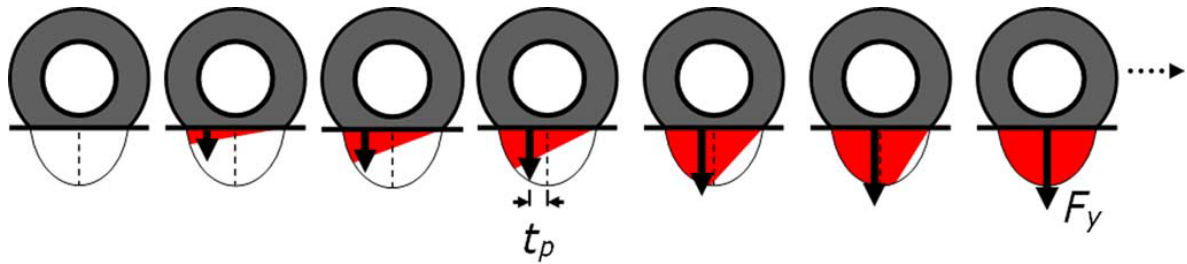


**Figure 1-4:** Decrease in pneumatic trail ( $t_p$ ) with increasing lateral force [12]

People driving passenger cars will notice the increasing steering torque with increasing lateral force. However, due to increased mechanical trail in modern cars it is hard for the inexperienced driver to feel the drop in aligning moment caused by a decrease in pneumatic trail [11]. This applies to FWD cars in particular because a driveshaft has to drive the steered wheels. To avoid the requirement for a large elongation of the driveshaft as the wheel rotates the kingpin offset has to be limited. The introduction of powersteering allows a suspension design with larger caster angles but the downside is that this will mask the drop in aligning moment as the tire limit is approached. By using wheel load sensing we hope to measure the lateral force and the aligning moment of the tires. The drop in aligning moment as the tires approach the limit can then be amplified and provided as additional feedback to the driver without limiting the suspension design or changing other vehicle handling characteristics. This will be of particular interest when vehicles become steer-by-wire.

The literature study showed that next to an increase in safety, the feedback might also help to increase driving pleasure and comfort. The thesis work is a follow-up study based on the Haptic Support Near the Limits (HSNL) system [4]. The HSNL system used a model based

approach to amplify the drop in aligning moment on the steering wheel. This can be improved by measuring the wheel loads with Load Sensing Bearings (LSBs). Identification of the forces in three directions has been done successfully and the focus for this thesis is on identification of the lateral force and aligning moment.

## 1-3 Content

The work in this thesis can be divided in two parts. The first part consists of a description of the LSBs that are developed by SKF for use in the Opel Astra at the Prodrive testtrack. It covers the experiments done and results used to filter- and calibrate the LSBs using the VEHICLE LOad Sensor (VELOS) measurement wheel. The goal is to obtain a good estimate of the lateral force and the aligning moment using measurements from the LSBs.

The second part contains a description of the used model to derive the signal for the haptic feedback electric motor from the measurements with the LSB. It describes the experiments done with test subjects with- and without haptic feedback on the steering wheel and the results derived from these experiments. A comparison is made with the results obtained in the HSNL study [4]. The thesis ends with a conclusion and recommendations for future work.

## 1-4 Hypothesis

The goal is to provide drivers with better haptic feedback on the steering wheel when a vehicle approaches its handling limits during cornering. This is a difficult task since the handling limits depend on the friction of the tires with the road surface which is constantly changing. As described in [8] the decrease in pneumatic trail of the tires and corresponding drop in aligning moment offers a mechanism to determine when the lateral force of the tires almost saturates, before it actually does. The hypothesis for this thesis work is:

**Measuring the lateral force and aligning moment of the tires with LSBs and providing the drop in aligning moment as haptic feedback on the steering wheel will increase driving pleasure and comfort and increases safety by preventing the driver from generating inputs leading to terminal understeer.**

## 1-5 Stakeholders

The project is a collaboration between the Delft University of Technology (TU Delft), SKF and Prodrive. It is a graduation project for the master in Mechanical Engineering (ME) with track Control Engineering (CE) and specialisation in Automotive at the TU Delft. The TU Delft provides the needed support and facilities. SKF provides an Opel Astra instrumented with sensors and haptic feedback system on the steering wheel and SKF provides LSBs to be mounted in the Opel Astra and corresponding support if needed. Prodrive provides the facilities to work in the office, the workshop and possibly the test track and provides support with instrumentation as well as content.

## Load sensing bearings

### 2-1 Description

#### 2-1-1 Bearing

Both original front wheel bearings of the Opel Astra used for testing are replaced with Load Sensing Bearings (LSBs) developed by SKF. The front wheel bearings used in the Opel Astra are double row ball bearings with pitch circle diameter of  $62\text{ mm}$  containing two rows of 16 equally spaced balls each with a diameter of  $11.112\text{ mm}$ , see Appendix A. The bearing is of type *BAR – 0050 AB* and is not the same as the rear wheel bearing because the vehicle has a front wheel drive configuration. The bearing is fixed with three bolts to the knuckle and has a five bolt mounting to the rim, see Figure 2-1. To develop a LSB the original bearing is modified and instrumented with sensors to measure the bearing deformation as a force is applied. A common way to measure the deformation is with strain gauges and in previous examples also eddy current sensors are used [13]. For the Opel Astra LSBs are developed with a combination of strain gauges and hall effect sensors. A note must be made that these LSBs are developed as a prototype for research purposes and hence do not meet industry standards in terms of production quality.



Figure 2-1: LSB drawing and photograph left- and right front

### 2-1-2 Strain gauges

SKF mounted three strain gauges to the flange of the bearing between the three attachment points to the knuckle. Figure 2-1 shows the position of the strain gauges, one at the bottom and the other two left- and right at 60 degrees from the top. Figure 2-2 shows one of the strain gauges mounted on the flange of the left front wheel bearing. The strain gauge signal is very small, measured in  $mV$  and very sensitive to noise and temperature because the strain gauges are wired to a quarter wheatstone bridge. The sensitive strain signals are transmitted to an amplifier / conditioner which is mounted under the bonnet, see Figure 2-4e. This amplifier is powered with 24 V from a 12 V power supply with a 12 V to 24 V DC/DC converter in between. Because the amplifier only accepts full bridges the quarter bridge for the single active strain gauge on the bearing is completed in the connectors by applying precision resistors, see Appendix B.

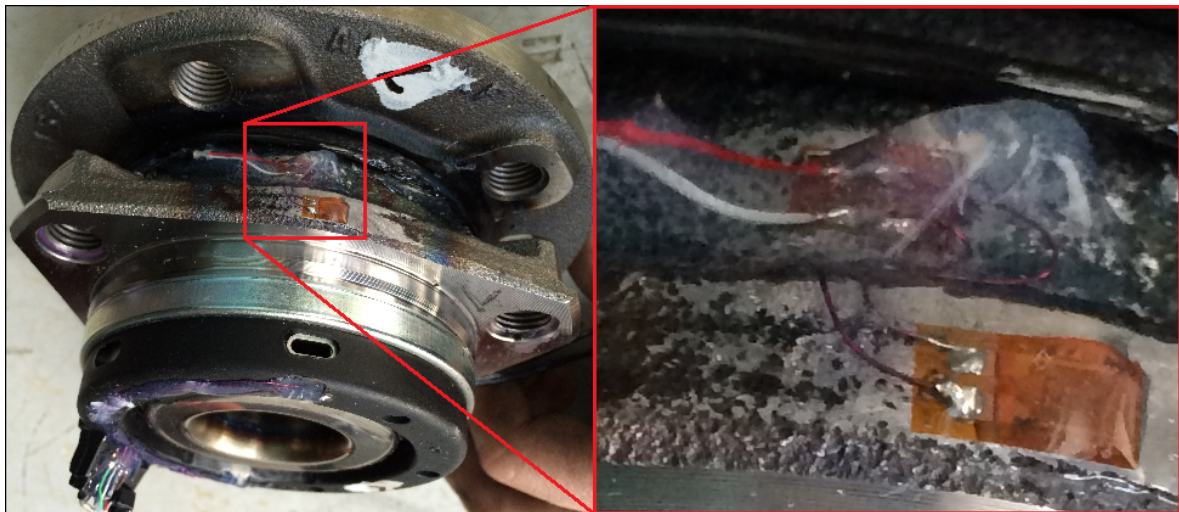


Figure 2-2: Strain gauge on left front LSB for Opel Astra

### 2-1-3 Hall effect sensors

Strain gauges measure the deformation of the bearing material. However, forces in two opposite directions can both cause the bearing to extend and with strain gauges only it is not possible to determine the direction of the force. In previous experiments eddy current sensors have been used to be able to measure the direction of the forces. The LSBs developed for the Opel Astra are instrumented with two hall effect sensors to measure tilting movements of the Anti-lock Braking System (ABS) ring. These hall effect sensors are placed at the top and bottom of the bearing as can be seen in Figure 2-1. They measure the distance between the fixed bearing housing and the rotating ABS ring. A lateral force will cause the ring to tilt a bit in one direction and the direction of the force can be determined from the displacement measured with the hall effect sensors. The hall effect sensors might also be used to measure the forces- and moments acting on the bearing. Although the results of the hall effect sensors are analyzed, the focus for this thesis will be on reconstruction of the lateral force and aligning moment from the bearing deformation measured with strain gauges.



### 2-1-4 BEaring Test SYstem (BETSY)

Calibration can be done on a test rig at SKF: BETSY. The work done by [14] showed us that it is best to calibrate the bearing-knuckle assembly as a whole because the compliant environment changes the force-strain relation compared to a rigid calibration. BETSY can apply forces and moments up to 15  $kN$  and 2.5  $kNm$  in 5 degrees of freedom [13]. This allows different forces- and moments to be applied and the strains can be measured to obtain the correct relations. The inverse of these relations can then be used in the application to calculate the forces- and moments from the measured combination of strains. The LSBs used in the Opel Astra are tested on BETSY as can be seen in Figure 2-3 but the calibration is done with measurements from the car using the VEHICLE LOad Sensor (VELOS) measurement wheel.

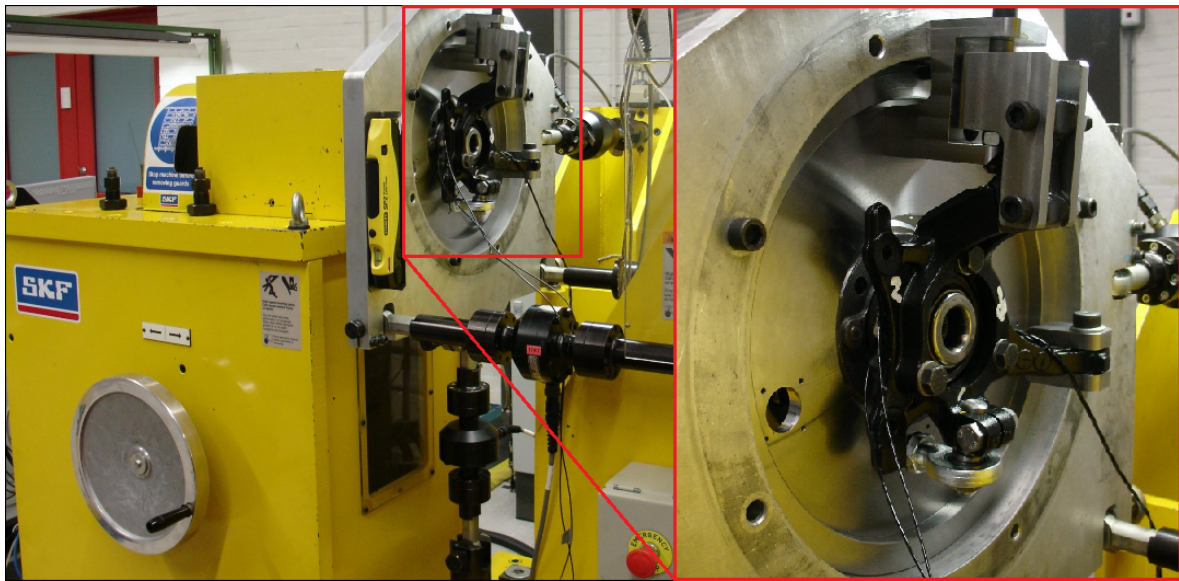


Figure 2-3: LSB with knuckle on BETSY for testing and controlled calibration

## 2-2 Experiments

### 2-2-1 Goal

The first experiments with the LSBs are done with the VELOS measurement wheel on the car. As described in section 2-3-1 this measurement wheel provides measurements of all wheel forces and moments. These measurements can be used afterwards to identify a model which reconstructs the forces- and moments from measurements with the LSBs. Section 2-3-3 shows that a linear model is able to describe the main dynamics. The strain gauge- and hall sensor signals are analyzed separately and different models are derived. A combined model is another possibility but is less feasible from a cost- and manufacturing point of view and will not be investigated now.

A Multiple Linear Regression Analysis (MLRA) is used to estimate the coefficients of this linear model ( $n = 1$ ) [13]. This is the most widely used technique in statistics and provides an easy solution to estimate the coefficients of a linear model [15]. The MLRA optimizes the cost function below with least squares. The function looks a bit different from the one given in [8] because the LSBs for the Opel Astra each have three strain gauges instead of six. The goal for this thesis is to provide better haptic feedback on the steering wheel by looking at the lateral force- and the aligning moment and therefore the focus will be on identifying a linear model to reconstruct these two.

$$\min_{\beta_0 \in \mathbb{R}^{2 \times 1}, \beta_l \in \mathbb{R}^{2 \times 3}} \sum_{k=1}^N \|FM - \beta_0 - \sum_{l=1}^n (\beta_l \epsilon^l)\|$$

$$FM = \begin{bmatrix} F_{y,t_k} \\ M_{z,t_k} \end{bmatrix} \quad \beta_0 = \begin{bmatrix} \beta_{0,F_y} \\ \beta_{0,M_z} \end{bmatrix} \quad \epsilon^l = \begin{bmatrix} \epsilon_{1,t_k}^l \\ \epsilon_{2,t_k}^l \\ \epsilon_{3,t_k}^l \end{bmatrix}$$

$$\beta_l = \begin{bmatrix} \beta_{l,1,F_y} & \beta_{l,2,F_y} & \beta_{l,3,F_y} \\ \beta_{l,1,M_z} & \beta_{l,2,M_z} & \beta_{l,3,M_z} \end{bmatrix}$$

### 2-2-2 Instrumentation

The Opel Astra is instrumented to measure vehicle states and driver inputs and provide haptic feedback on the steering wheel [4]. The haptic feedback is provided by a Maxon Brushed 36 V Direct Current (DC) electric motor on the steering wheel with 200 W power controlled through a Maxon 500 W motor controller. A belt from Maedler in combination with pulleys is used to transfer the torque from the motor to the steering column as can be seen in Figure 2-4c. A 100 Hz dual antenna Global Positioning System (GPS) system from Racelogic type *VBSS100SL* shown in Figure 2-4b will be used to measure longitudinal and lateral velocity and calculate slip angles. Inertial states including accelerations and rotational rates are measured with breakout boards from Sparkfun and with the GPS / Inertial Measurement Unit (IMU) unit from Racelogic, both displayed in Figure 2-4a. To provide accurate results, the IMU units have to be mounted in the Center Of Gravity (COG) which is close to the hand brake for the Opel Astra. Wheel encoder signals are tapped from the car's ABS unit and strain gauges are attached to the steering column to measure steering torque. In the steering wheel there is also a sensor to measure the steering wheel angle. Wheel forces and moments are measured with the VELOS measurement wheel from Kistler shown in Figure 2-4d and with the LSBs from SKF. The VELOS measurement wheel instrumentation as well as the strain gauge amplifier contain a 100 Hz low-pass hardware filter. All signals are sent to the dSPACE 300 MHz MicroAutoBoX (MABX) 1401 / 1501. The signals from the VELOS measurement wheel are first put on the Controller Area Network (CAN) bus by the *VBADC03* analogue input module from Racelogic because the MABX has only 16 analogue inputs. The Racelogic GPS / IMU unit also communicates with the MABX over CAN. Interfacing and data storage is done through an Intel: *D510MO* 1.66 GHz Dual Core Atom Mini-ITX motherboard. Data is logged at a sampling rate of 1000 Hz. Logging automatically starts once a vehicle velocity of 3 m/s is reached and stops once the velocity drops below this value. An overview of the logged signals, vehicle states and driver inputs is given here:

- Driver steering torque
- Steering wheel angle
- Throttle position
- Lateral acceleration
- Longitudinal acceleration
- Vehicle velocity
- Body slip angle
- Yaw-rate
- Latitude
- Longitude
- Heading
- Wheelspeeds
- VELOS measurement wheel signals
- LSB strains
- LSB hall effect sensors

The data is stored on disk using the "Stream-to-disk" option in the dSPACE Control desk software with a window of 2 seconds. This means that the data is collected in the memory and written to disk every 2 seconds preventing memory errors and allowing long datasets.

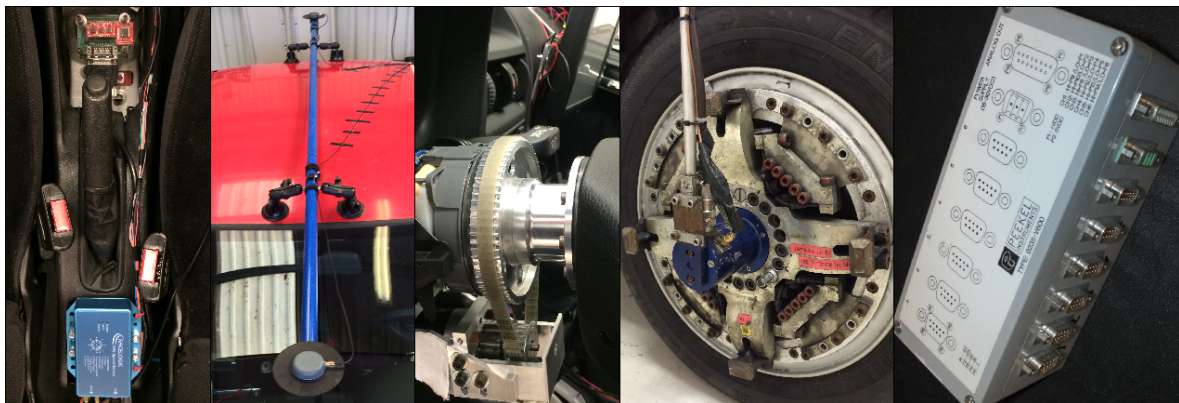


**Figure 2-4:** Instrumentation in the Opel Astra: a) IMU units b) Dual Antenna GPS c) Electric motor on steering column d) VELOS measurement wheel e) LSB strain gauge amplifier

### 2-2-3 Calibration procedure

The experiments are done at the Prodrive test track in Kenilworth Warwickshire, see Figure 2-5. This track has different facilities including high  $\mu$  tarmac surfaces ( $\mu = 0.9 - 1$ ) and low  $\mu$  surfaces ( $\mu = 0.25 - 0.3$ ) made wet with sprinklers to simulate driving on snow and ice. There are two low  $\mu$  surfaces: a straight to test accelerating and braking performance and a circle to test cornering behaviour. The identification is performed on the high  $\mu$  tarmac because the amplitudes of the forces- and moments are high. First all experiments are done with the VELOS measurement wheel on the left side to identify the parameters for the left LSB and the experiments are repeated with the measurement wheel mounted on the right side. To obtain data from different maneuvers the following datasets are logged:



**Figure 2-5:** Prodrive test track: high and low  $\mu$  circles and straights

5x clockwise circle in second gear  
 5x counterclockwise circle in second gear  
 5x clockwise circle in third gear  
 5x counterclockwise circle in third gear  
 5x straight line accelerating heavy braking  
 5x straight line accelerating coast down  
 5x slalom

For the circular datasets the test method with constant steering-wheel angle is used [16]. This means that the steering wheel angle is kept constant and the speed is slowly increased. The International Organization for Standardization (ISO) standard recommends steering wheel angles of  $\pm 20$  degrees and velocity increments of  $20 \text{ km/h}$  up to  $100 \text{ km/h}$ . Unfortunately the width of the track was limited so for the test the steering wheel angle is higher and the test speed is limited.

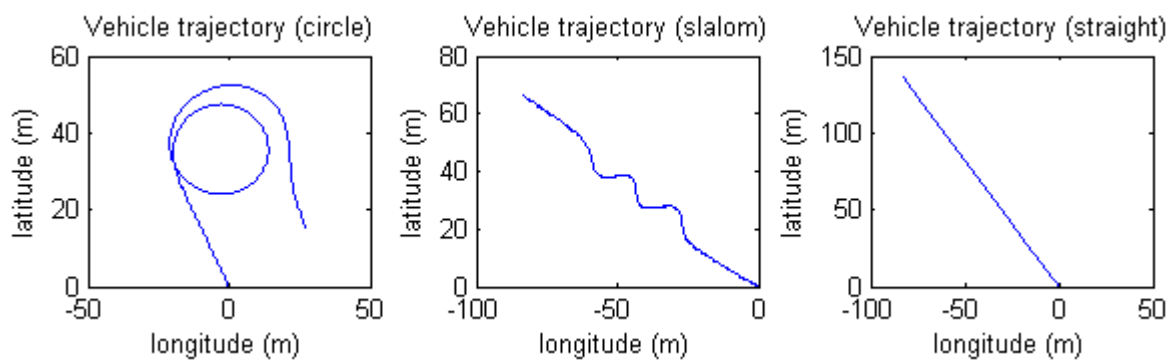


**Figure 2-6:** Vehicle trajectories for three different maneuvers: circle, slalom and straight

Figure 2-6 shows a top view of the different maneuvers as logged with the GPS system. This controlled combination of datasets with steady-state as well as dynamic forces- and moments allows easy data analysis and in the mean time provides a rich input for identification. This thesis will focus mainly on steady-state cornering behaviour but it is still useful to use some longitudinal data in the identification. This prevents strong disturbance of the model by high longitudinal forces and makes the model more robust.

## 2-3 Results

### 2-3-1 Measurements

#### VELOS measurement wheel

In Figure 2-7 raw measurements from the VELOS measurement wheel mounted on the left front side are displayed. These are measurements from one of the clockwise datasets in second gear and this dataset will be used in most figures in this thesis to show the different results. The signals measured here are still in the wheel rotational frame and have to be translated to a fixed wheel coordinate system. This is done using these formulas [13][17]:

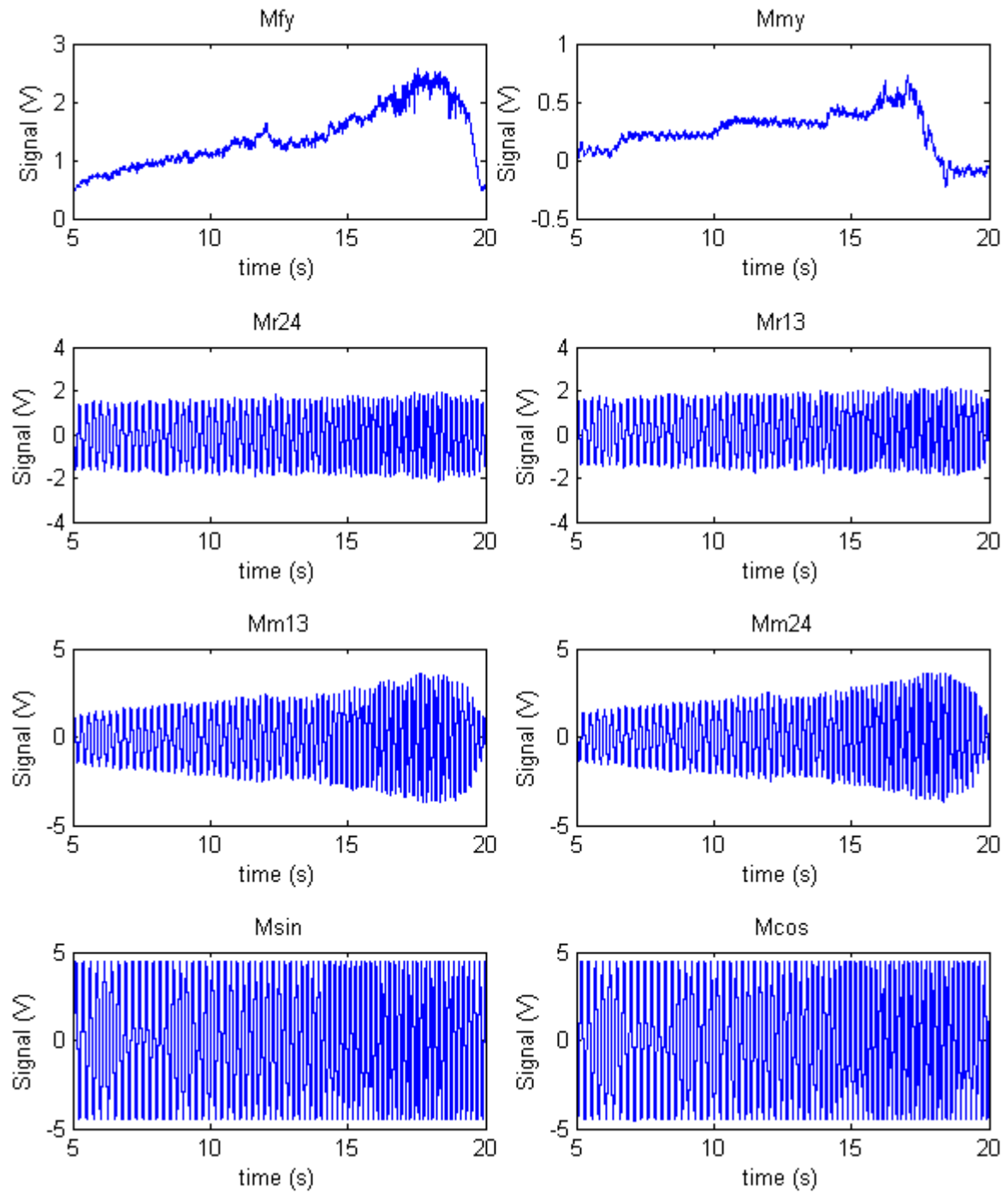
$$\begin{aligned}
 F_y &= K(fy) \cdot Mfy \\
 M_y &= K(my) \cdot Mmy \\
 F_x &= Mr13 \cdot K(r13) \cdot Msin \cdot K(sin) - Mr24 \cdot K(r24) \cdot Mcos \cdot K(cos) \\
 F_z &= -Mr13 \cdot K(r13) \cdot Mcos \cdot K(cos) - Mr24 \cdot K(r24) \cdot Msin \cdot K(sin) \\
 M_x &= -Mm13 \cdot K(m13) \cdot Mcos \cdot K(cos) - Mm24 \cdot K(m24) \cdot Msin \cdot K(sin) \\
 M_z &= -Mm13 \cdot K(m13) \cdot Msin \cdot K(sin) + Mm24 \cdot K(m24) \cdot Mcos \cdot K(cos)
 \end{aligned}$$

**Table 2-1:** VELOS measurement wheel calibration factors

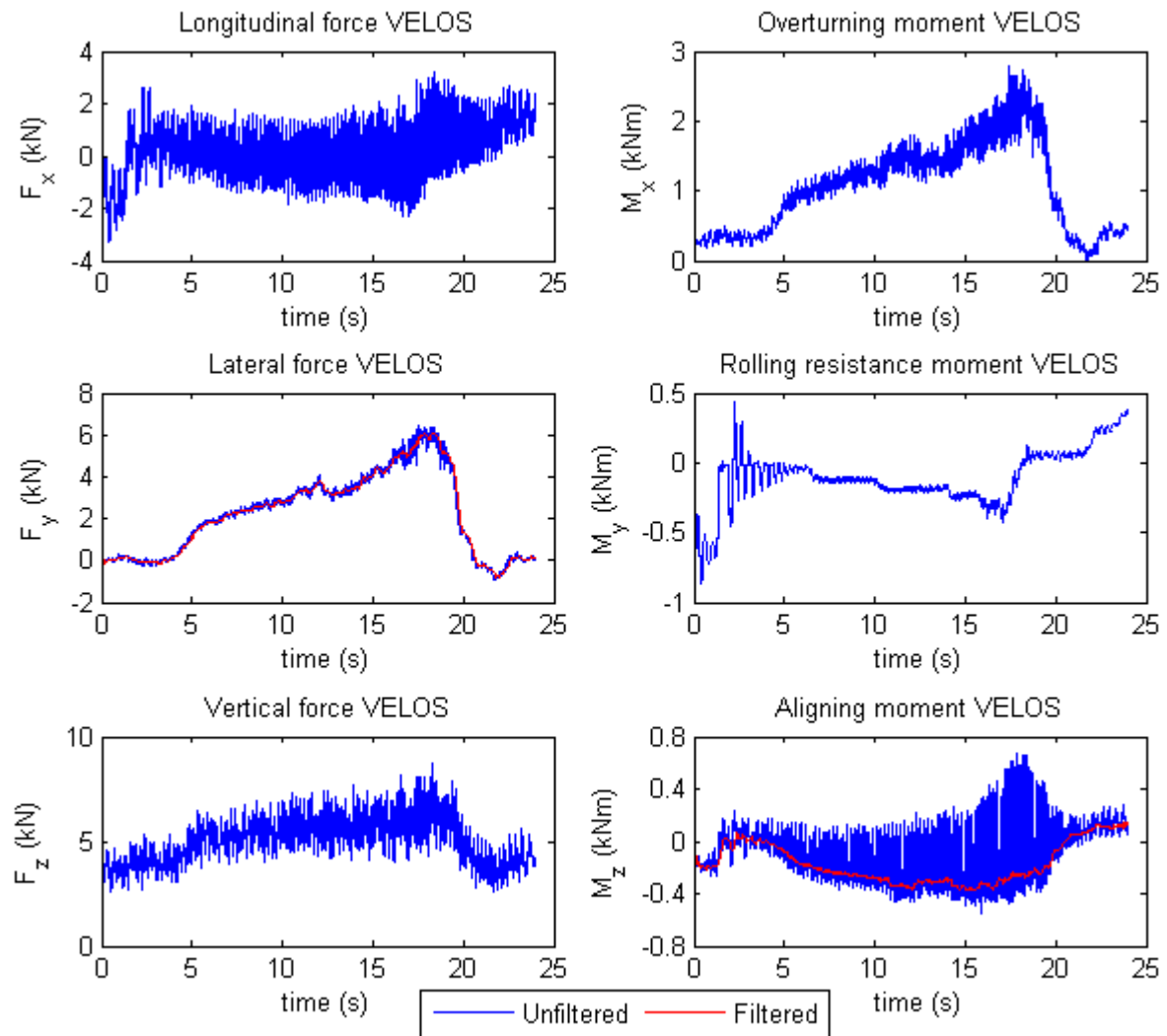
K(fy)	2.530 N/mV
K(r13)	3.476 N/mV
K(r24)	3.368 N/mV
K(my)	0.580 Nm/mV
K(m13)	0.638 Nm/mV
K(m24)	0.683 Nm/mV
K(sin)	0.222 1/mV
K(cos)	0.222 1/mV

Figure 2-8 shows the reconstructed forces- and moments which follow after applying the formulas to the raw measurement data. Notice that the data for  $F_y$  is much less oscillating than the data for  $M_z$ . This can be explained by looking at the measurement wheel construction and the applied formulas. The calculation for  $F_y$  does not contain  $\sin$  and  $\cos$  components and does not need to be translated from rotational to fixed coordinate system. To improve the measurements the oscillations can be removed by filtering as will be explained in section 2-3-2. Notice that between 15 and 20 seconds the lateral force is still increasing while the aligning moment drops in amplitude. This is an indication that the vehicle is driving towards the limit and will be used later to provide haptic feedback on the steering wheel.





**Figure 2-7:** Raw signals measured with VELOS measurement wheel mounted on the left front for clockwise circle maneuver



**Figure 2-8:** Forces and moments measured with VELOS measurement wheel mounted on the left front for clockwise circle maneuver

### Strain gauges

The strains measured with the LSBs for the left- and right front wheel for the same clockwise maneuver as before are shown in Figure 2-9. Strain  $4_L$ ,  $5_L$  and  $6_L$  are equal to strains 1, 2 and 3 on the left side in Figure 2-1 respectively but are renamed to avoid confusion between left- and right. The unfiltered signals are heavily oscillating but can be filtered to improve the measurements as will be explained in detail in section 2-3-2. Notice that some strain signals have a similar shape to the measured lateral force- and aligning moment with the VELOS measurement wheel. This already is an indication that the strains indeed contain the desired information on the tire-road forces. In section 2-3-3 the reconstruction of the lateral force- and aligning moment by using a combination of these strains is explained.

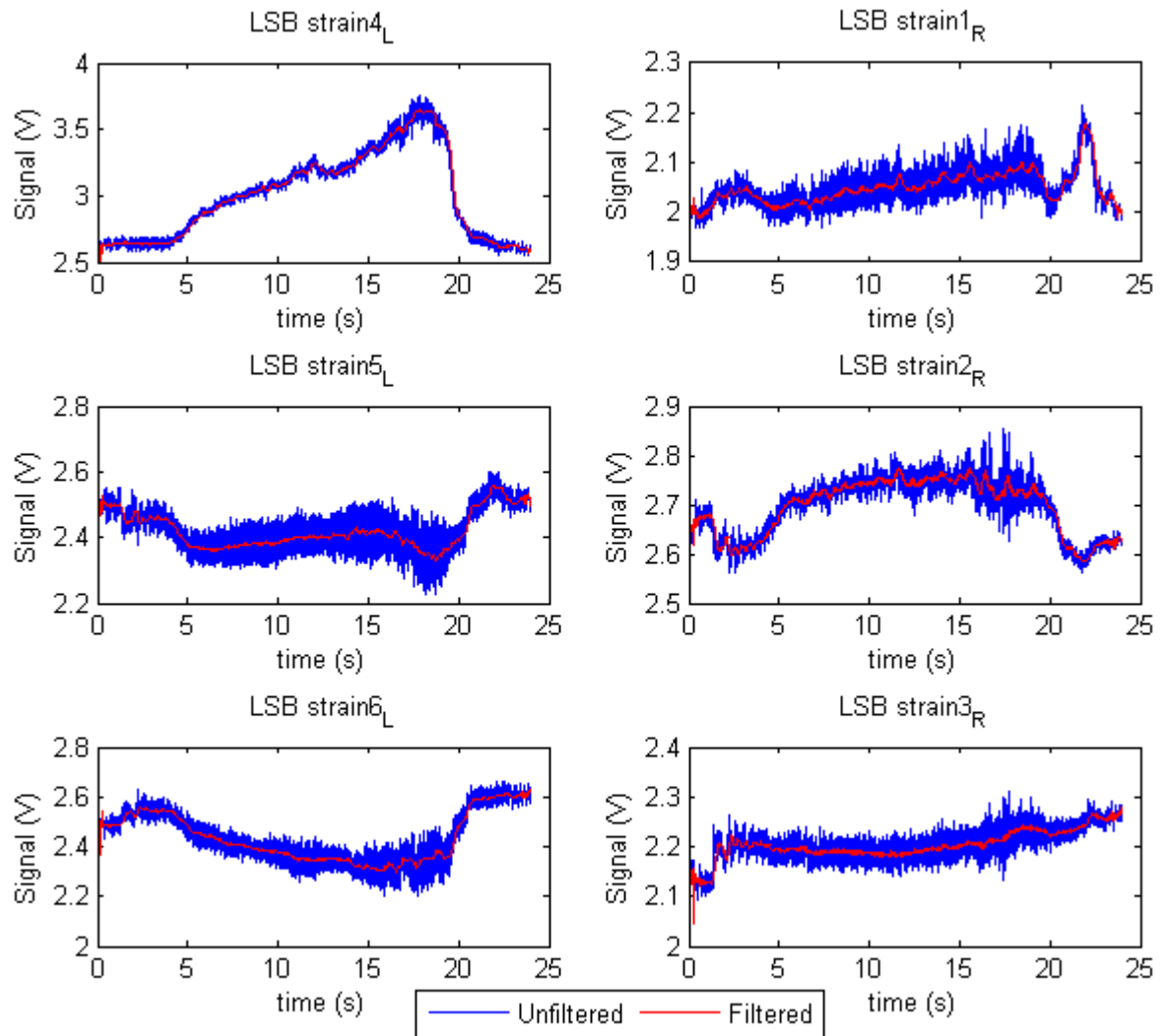


**Figure 2-9:** Unfiltered and filtered strains measured with LSBs for clockwise circle maneuver

### Hall effect sensors

The raw data from the hall effect sensors is given in Figure 2-10. The signals are heavily oscillating because the hall effect sensors are looking at a tilting movement of the ABS ring and this ring has holes in it to measure the wheel speed. In [13] an algorithm is described to identify if the hall effect sensor is looking at the ring or through a hole in the ring, to obtain the displacement of the ABS ring from the measurements. However, for the measurements with the Opel Astra a different filtering procedure described in section 2-3-2 is used to show the potential of the measurements with the hall effect sensors. The filtered hall effect signals can be found in Figure 2-11. If this is compared with the results from the VELOS measurement wheel in Figure 2-8 it becomes clear that indeed the hall effect sensors contain useful information. In section 2-3-3 the reconstruction of the lateral force- and aligning moment by using a combination of these hall effect sensors is explained.



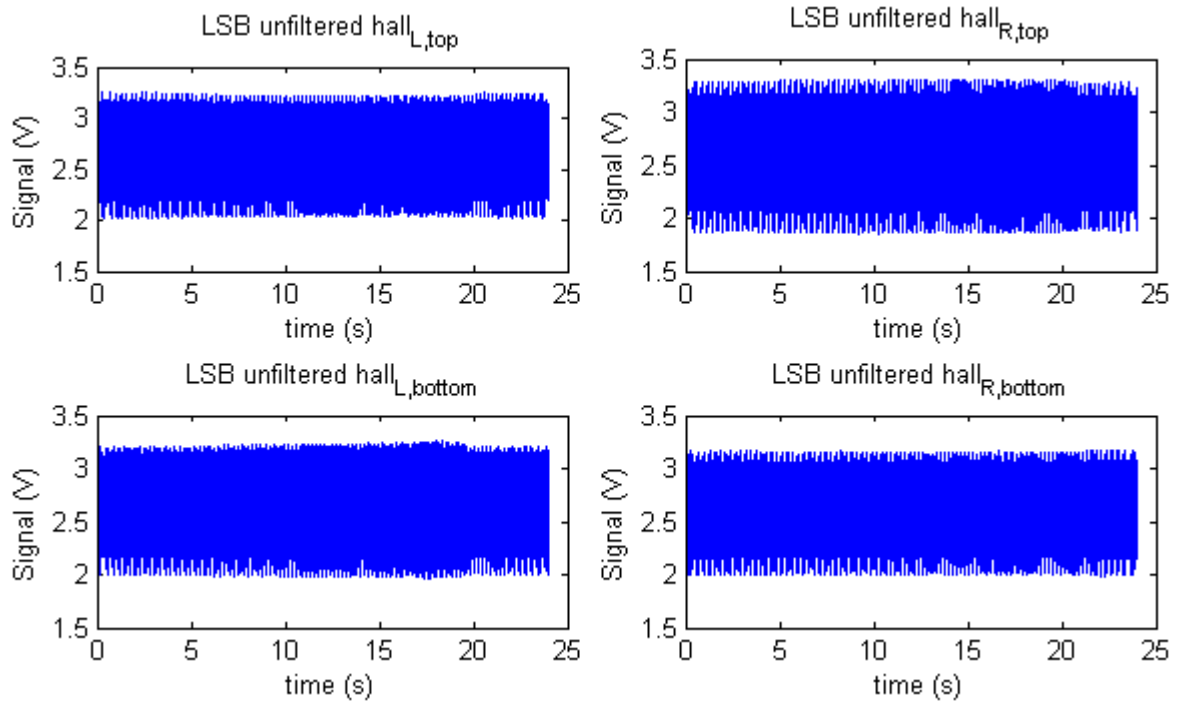


**Figure 2-10:** Unfiltered hall effect signals measured with LSBs for clockwise circle maneuver

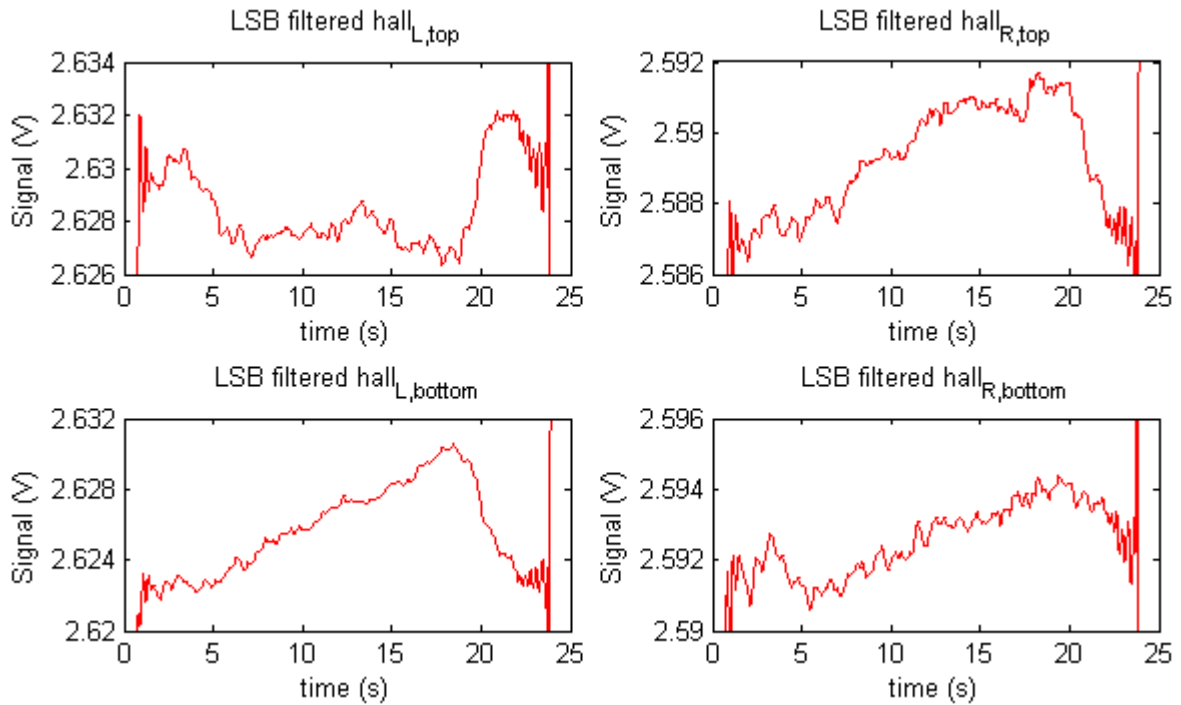


**Figure 2-11:** Filtered hall effect signals measured with LSBs for clockwise circle maneuver

### 2-3-2 Filtering

#### VELOS measurement wheel

Figure 2-8 shows unfiltered and filtered signals from the VELOS measurement wheel. This section explains the filtering procedure to get from the unfiltered signal to the filtered signal. Spectral analysis in Figure 2-12 reveals that the main frequency of disturbance for the VELOS measurement wheel is 4–6 Hz. Further analyzes from signals at different speeds tells us that this frequency is linked to the wheel rotational velocity which varies between 4–6 Hz. The disturbance at wheel rotational frequency can be caused by multiple reasons. First of all a small calibration error in the raw signals from the measurement wheel will cause oscillations when translating from a rotational to a static coordinate system. As described in [13] this disturbance might be caused "by variations in radial stiffness" although in this research the Spinning Wheel Integrated Force Transducer (SWIFT) instead of the VELOS measurement wheel was used. There is probably also an unbalance in the wheel causing oscillations at the wheel rotational frequency. This can all be filtered by applying a velocity dependent notch filter as described in [8] and given below. The  $r_{value}$  determines the width of the notch filter and is found by trial-and-error. A value of 0.97 was found to give good results in this case.

$$H(z) = K_\mu \cdot \frac{1 + \omega_d z^{-1} + z^{-2}}{1 + r_{value} \omega_d z^{-1} + r_{value}^2 z^{-2}}$$

$$K_\mu = \frac{1 + r_{value} \omega_d + r_{value}^2}{2 + \omega_d}$$

$$\omega_d = -2 \cos(\omega_f \cdot T_s)$$

The frequency spectrum of the aligning moment also shows a smaller peak around 12 Hz. Further analysis at different speeds shows that this component is linked to twice the rotational velocity of the wheel. According to [13] this might also be caused by variations in radial stiffness of the measurement wheel. A disturbance at four times the wheel rotational frequency could then also be expected but is small in these measurements with the measurement wheel. Still, the signals can be improved by applying a velocity dependent notch filter with a frequency of two- and four times the wheel rotational frequency as well. A second order 5 Hz low-pass filter is used to remove other high frequency noise.

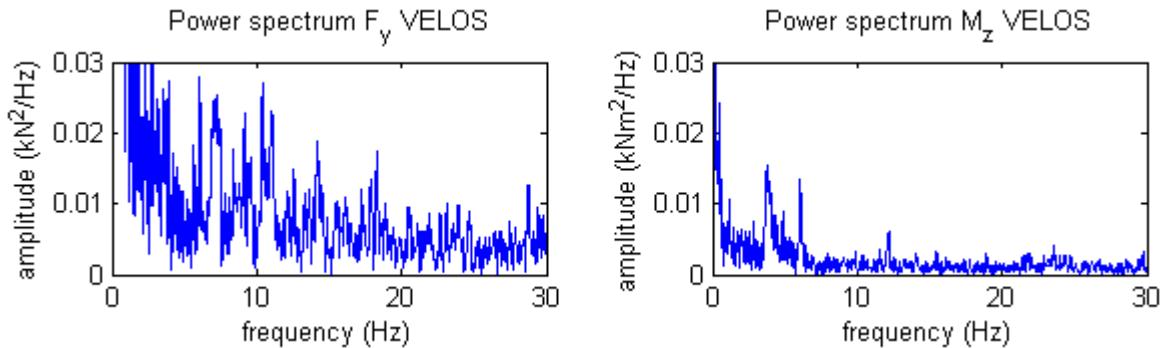


**Figure 2-12:** Power spectrum of lateral force and aligning moment measured with VELOS

### Strain gauges

The spectral analysis of the strains in Figure 2-13 shows different peaks. One of the clearest peaks is around 40  $Hz$ . Analysis shows that this peak is equal to the ball-pass frequency in the bearing which can be calculated from the wheel rotational velocity using the theory of planetary gearboxes [13].

$$\begin{aligned}
 D_{ir}\omega_{ir} + D_{or}\omega_{or} &= (D_{or} + D_{ir}) \cdot \omega_{ballcarrier} \\
 \omega_{ballcarrier} &= \omega_{ir} \cdot \frac{D_{ir}}{D_{or} + D_{ir}}, \quad (\omega_{or} = 0) \\
 \omega_{ir} &= \omega_{wheel} \\
 \omega_{ballpass} &= N \cdot \omega_{ballcarrier} \\
 \omega_{ballpass} &= N \cdot \frac{D_{ir}}{D_{or} + D_{ir}} \cdot \omega_{wheel}
 \end{aligned}$$

The parameters can be found by looking at the bearing geometry in Appendix A, the number of balls in one row of the bearing ( $N$ ) and the inner- and outer diameter of the bearing ball carrier ( $D_{ir}$ ) and ( $D_{or}$ ). This yields the ballpass frequency as a constant multiplied with the wheel frequency.

$$\begin{aligned}
 N &= 16 \\
 D_{ir} &= 62 - 11.112 = 50.888 \text{ mm} \\
 D_{or} &= 62 + 11.112 = 73.112 \text{ mm} \\
 \omega_{ballpass} &= N \cdot \frac{D_{ir}}{D_{or} + D_{ir}} \cdot \omega_{wheel} \\
 \omega_{ballpass} &\approx 6.57 \cdot \omega_{wheel}
 \end{aligned}$$

With a wheel frequency of around 6  $Hz$  this explains the peak at 40  $Hz$ . The effect can be filtered again by using a velocity dependent notch filter. A closer look at the spectral analysis shows that again there are peaks around the wheel rotational frequency and twice the wheel rotational frequency. In this case also a clear peak at four times the wheel rotational velocity is visible. Applying velocity dependent notch filters at these frequencies also significantly improves the measured signal so these are applied here as well. Again a second order 5  $Hz$  low-pass filter is used on top of the velocity dependent notch filters. Figure 2-9 shows the raw- and filtered strains from one of the measurements of a clockwise circle maneuver. It is clear that the filtering is absolutely necessary and improves the signals a lot. This can be a problem for applications in commercial passenger vehicles because the available computational power might not be sufficient. For the experiments in this thesis it is not critical because enough computational power is available in the Opel Astra.

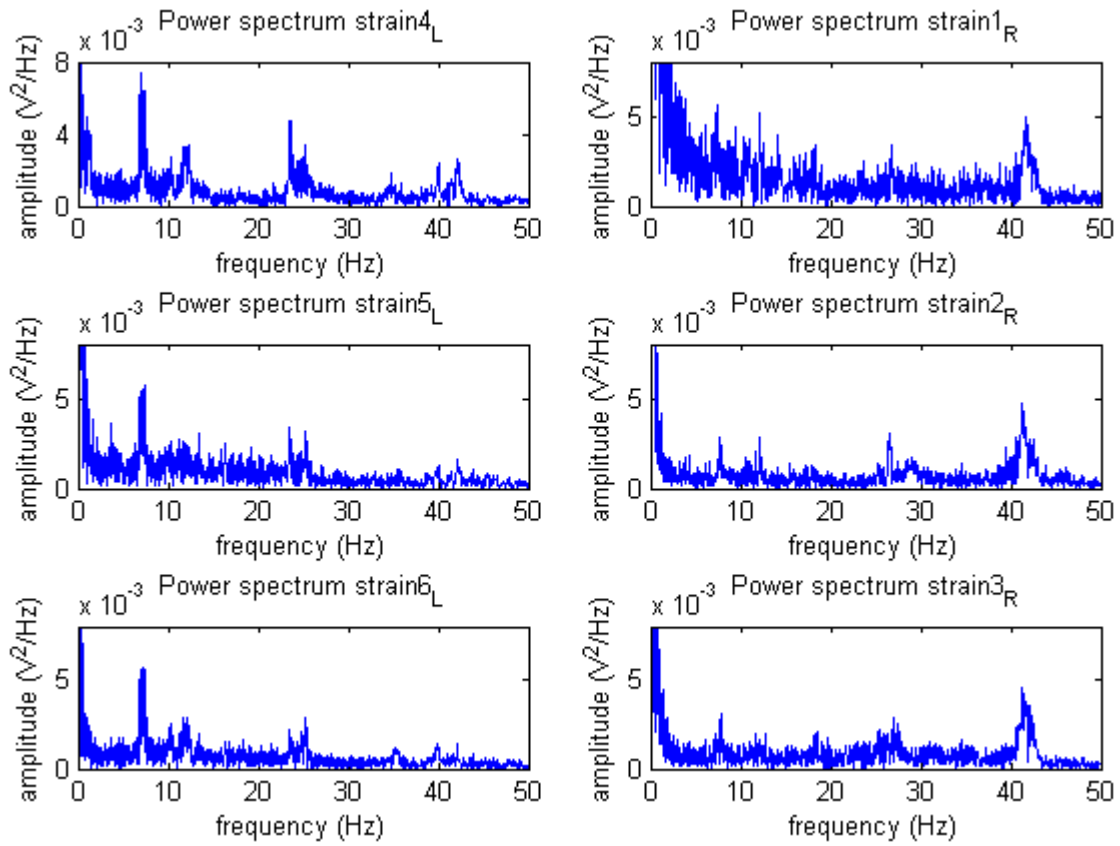


**Figure 2-13:** Power spectrum of strains measured with LSBs

### Hall effect sensors

The spectral analysis for the raw signals of the hall effect sensors is plotted for frequencies up to 250  $Hz$  instead of 50  $Hz$  in Figure 2-14. Reason for this is that the disturbances are at a much higher frequency than the wheel rotational frequency since the ABS ring has a lot of holes passing the sensor every time the wheel makes a full rotation. The number of holes in the ABS ring for the bearings in the Opel Astra is 29. Because the disturbances are at such a high frequency, a strong eighth order 5  $Hz$  low-pass filter will be used to remove the oscillations. Further analysis of the signals in the time domain shows there also is a strong frequency component of approximately 4.6 times the wheel rotational frequency. A possible explanation for this disturbance is that the ABS ring might be slightly warped. This can be caused for example due to the way the ABS ring is mounted. Since this frequency is not a lot higher than the low-pass filter frequency, again a velocity dependent notch filter at this frequency is used to remove the disturbance.

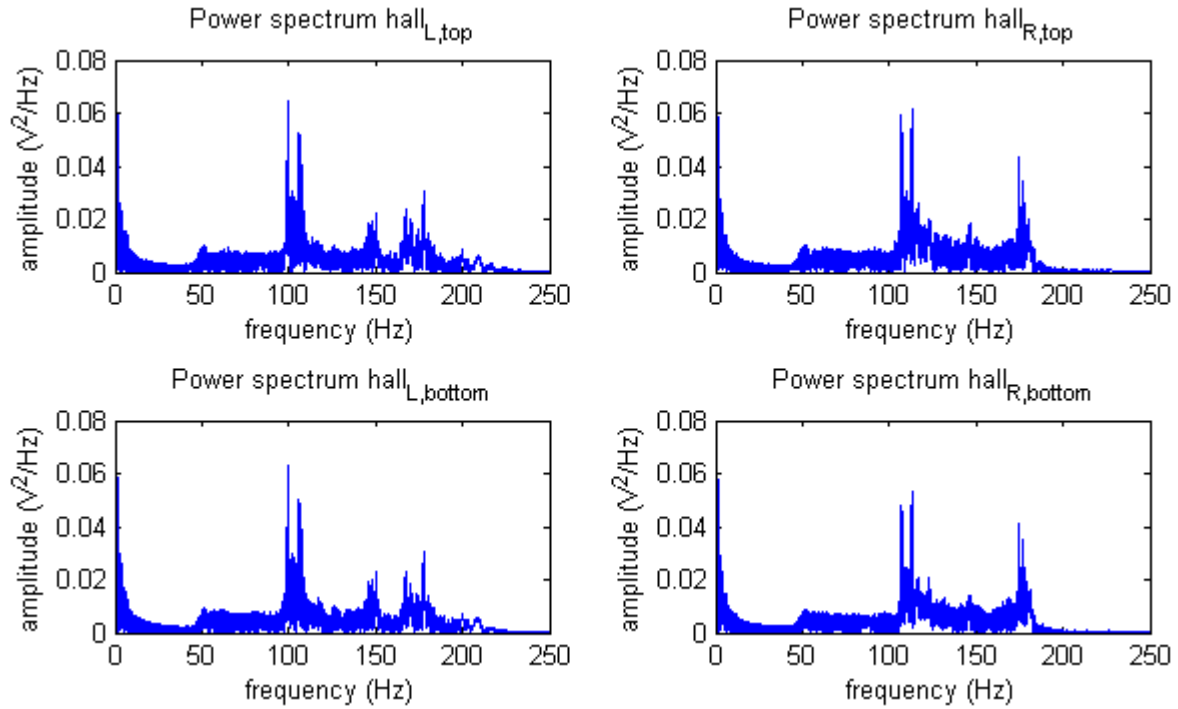


**Figure 2-14:** Power spectrum of hall signals measured with LSBs

### 2-3-3 System identification

#### Strain gauges

The filtered data from the 35 collected datasets for each front wheel is used to create a linear model using the MLRA given in Section 2-2-1. This MLRA finds the best fit of a linear combination of the three strain gauges to the data measured with the VELOS measurement wheel using a linear least squares algorithm. The focus is on finding a model for the lateral force and the aligning moment. Each dataset is detrended before the MLRA is done. This makes sure the linear trend is removed from each dataset and removes possible drift and static offsets in the data. The disadvantage of detrending is that the MLRA will not find values for the vector  $\beta_0$ . However, this will be solved in practice by zeroing the estimated lateral force and aligning moment if the vehicle velocity is zero. This accounts for drift and is a suitable solution for the short experiments that are performed. The found coefficients for the models of the lateral force and aligning moment of the left- and right front wheel are given below.

**Table 2-2:** Coefficients of LSB strain models

LEFT				RIGHT			
$\beta_{1,1,F_y}$	3.5122	$\beta_{1,1,M_z}$	0.12867	$\beta_{1,1,F_y}$	3.0653	$\beta_{1,1,M_z}$	-0.24279
$\beta_{1,2,F_y}$	-9.6082	$\beta_{1,2,M_z}$	-0.38636	$\beta_{1,2,F_y}$	-10.641	$\beta_{1,2,M_z}$	-0.36507
$\beta_{1,3,F_y}$	-4.1304	$\beta_{1,3,M_z}$	2.046	$\beta_{1,3,F_y}$	-1.8504	$\beta_{1,3,M_z}$	-2.6461

Figure 2-15 shows the model contribution of the three strains to the reconstruction of the lateral force- and aligning moment of the left front wheel. The lateral force estimation is based mainly on strain gauge  $\epsilon_1$  which is placed at the bottom of the bearing, see Figure 2-1. However, a vertical force will cause this strain gauge to deform a lot as well and large part of the deformation is probably the result of a change in vertical force caused by load transfer during cornering. Hence, it is questionable how good the estimation will be if the vertical force is fluctuating a lot for example if the vehicle drives over a bump. All three strain contributions are positive for the reconstruction of the lateral force.

The estimation of the aligning moment is based mainly on strain gauge  $\epsilon_3$  which is placed at 60 degrees from the top of the bearing to the rear, see Figure 2-1. The shape of this strain deformation is very similar to the estimation of the aligning moment. The strain gauge is placed between the attachment points of the upper ball joint and the tie rod, see Figure 1-2 and Figure 2-3. This makes sense since the load path of a moment around the vertical axis of the tire is mainly through the tie rod which is part of the steering system. The other two strain contributions are negative for the reconstruction of the aligning moment.

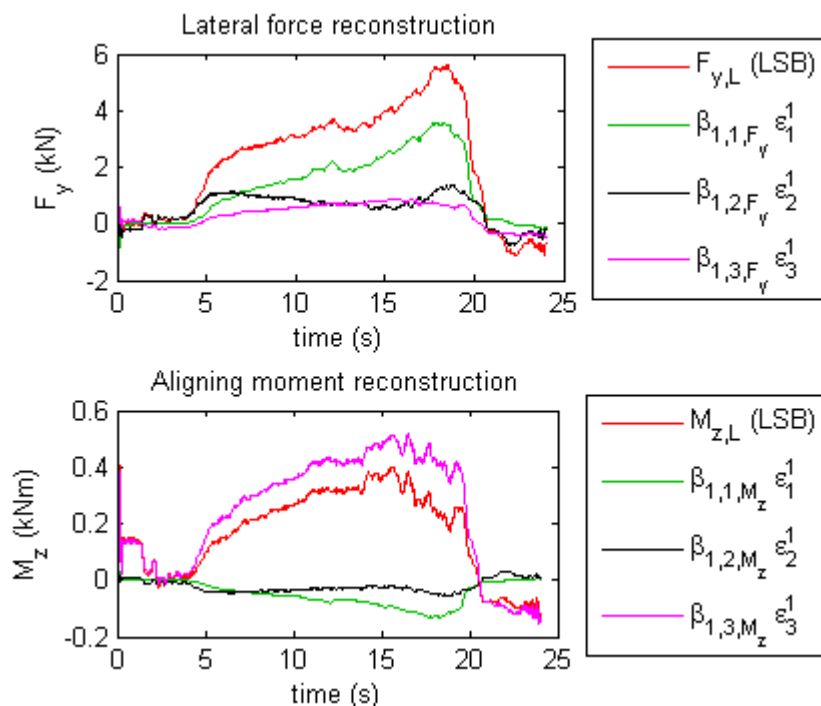


**Figure 2-15:** Strain contributions lateral force and aligning moment model

A comparison between the estimated force and aligning moment by the model and the signals measured with the VELOS measurement wheel is given in Figure 2-16. This shows a good match between the strain model estimation and the VELOS measurements in the time domain. The quality of the model is evaluated using Variance Accounted For (VAF) values and the auto- and cross-correlation tests later.

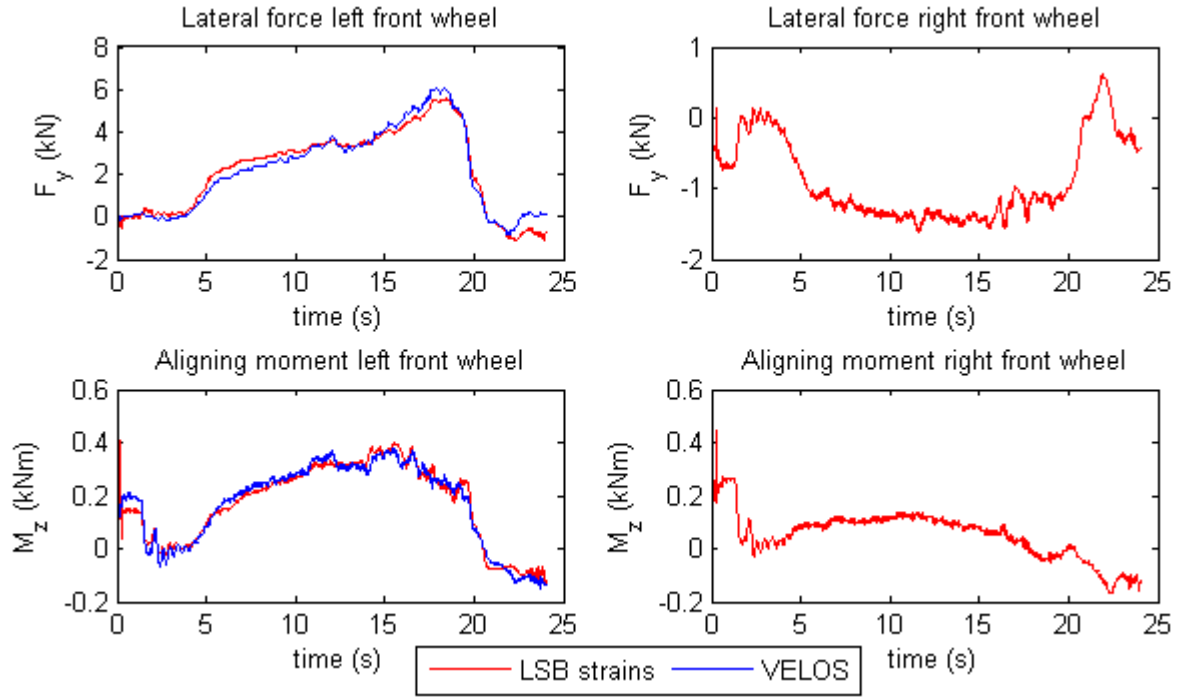


**Figure 2-16:** Lateral force and aligning moment strain model comparison with VELOS wheel

The used model is a first order model and the model might be improved by using a higher order model. A way to get a feeling of the needed model order is by looking at the singular values [18]. If a clear gap can be distinguished between two singular values this is an indication that the higher singular values are caused by noise and do not describe the dynamics. To do a singular value analysis, first the Hankel matrices of the input- and output have to be constructed:

$$U_{1,s,N} = \begin{bmatrix} u(0) & u(1) & \dots & u(N-1) \\ u(1) & u(2) & \dots & u(N) \\ \vdots & \vdots & \ddots & \vdots \\ u(s-1) & u(s) & \dots & u(N+s-2) \end{bmatrix}, Y_{1,s,N} = \begin{bmatrix} y(0) & y(1) & \dots & y(N-1) \\ y(1) & y(2) & \dots & y(N) \\ \vdots & \vdots & \ddots & \vdots \\ y(s-1) & u(s) & \dots & y(N+s-2) \end{bmatrix}$$

The value of  $s$  has to be chosen larger than the model order to be estimated and can only be found by trial-and-error. In general a value of twice the maximum model order to be estimated provides good results. A QR-factorization is applied which yields:

$$\begin{bmatrix} U_{1,s,N} \\ Y_{1,s,N} \end{bmatrix} = \begin{bmatrix} R_{11} & 0 \\ R_{21} & R_{22} \end{bmatrix} \cdot \begin{bmatrix} Q_1 \\ Q_2 \end{bmatrix}$$

A singular value analysis is done on the  $R_{22}$  matrix. This yields a Singular Value Decomposition (SVD) including the  $\Sigma$  matrix with the singular values on the diagonal.

$$R_{22} = U \Sigma V^T$$

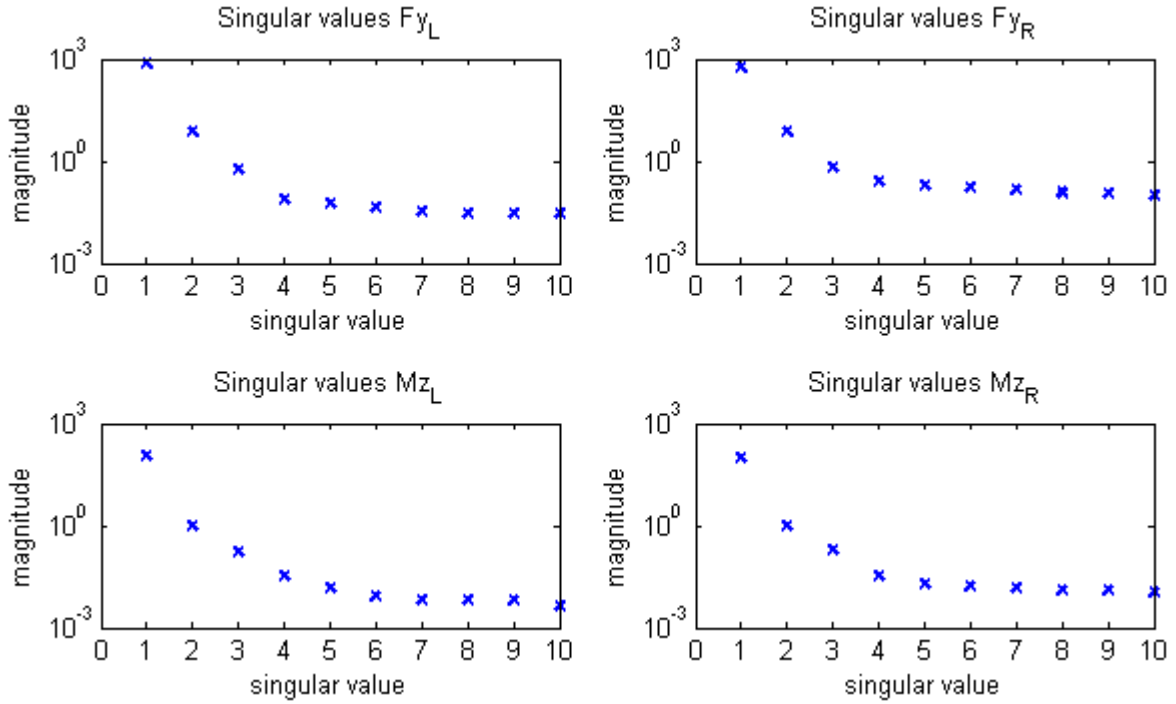


**Figure 2-17:** Singular values for strain inputs with lateral force and aligning moment

The first 10 singular values are plotted in Figure 2-17. It is difficult to see a clear gap between two of the singular values, but an important observation is that the first singular value is more than one order of magnitude higher than the other singular values. This is an indication that the first mode shape is dominant and that a first order model is already able to describe the main dynamics. To get a better idea of the quality of the model the VAF is evaluated for different maneuvers in Figure 2-18. The different maneuvers are the ones described in Section 2-2-3 and shown in Figure 2-6. The VAF is calculated with [18]:

$$VAF(y(k), \hat{y}(k, \theta)) = \max \left( 0, \left( 1 - \frac{\frac{1}{N} \sum_{k=1}^N \|y(k) - \hat{y}(k, \theta)\|_2^2}{\frac{1}{N} \sum_{k=1}^N \|y(k)\|_2^2} \right) \cdot 100\% \right)$$

A VAF value of 100 % means that the model estimate is exactly the same as the measured data. In practice this is not possible because there is always noise in the system and in the measurements. The VAF for the identified model is high, especially for the outside wheel during cornering since the lateral force is high in this case. The VAF is plotted for model orders 1 – 3 and is in most cases slightly larger for higher model orders. However, for the real-time estimation a first order model is chosen since this is less computationally demanding and the increase in VAF is not much for higher model orders.



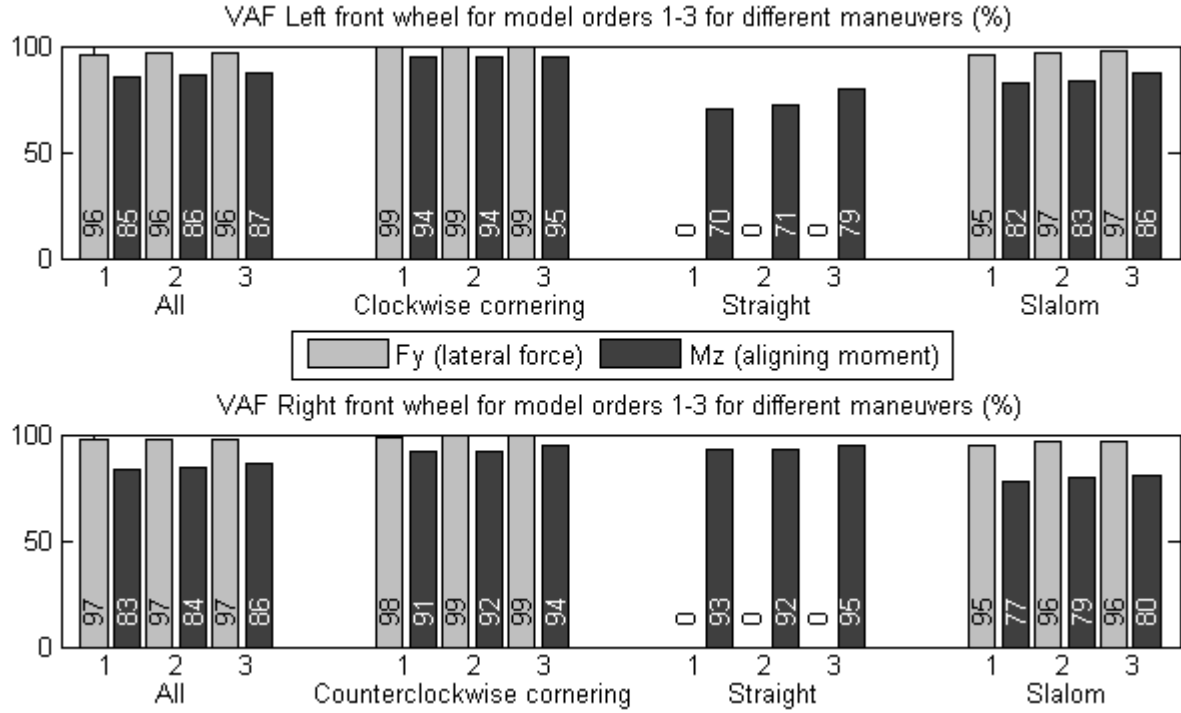


**Figure 2-18:** Variance Accounted For for model orders 1-3 for different maneuvers

A good way to validate a model is by looking at the autocorrelation of the residual (difference between model estimation and real measurements) and the cross-correlations between the inputs and the residual. With residual  $\hat{\epsilon}(k, \hat{\theta})$  the following two properties are evaluated [18]:

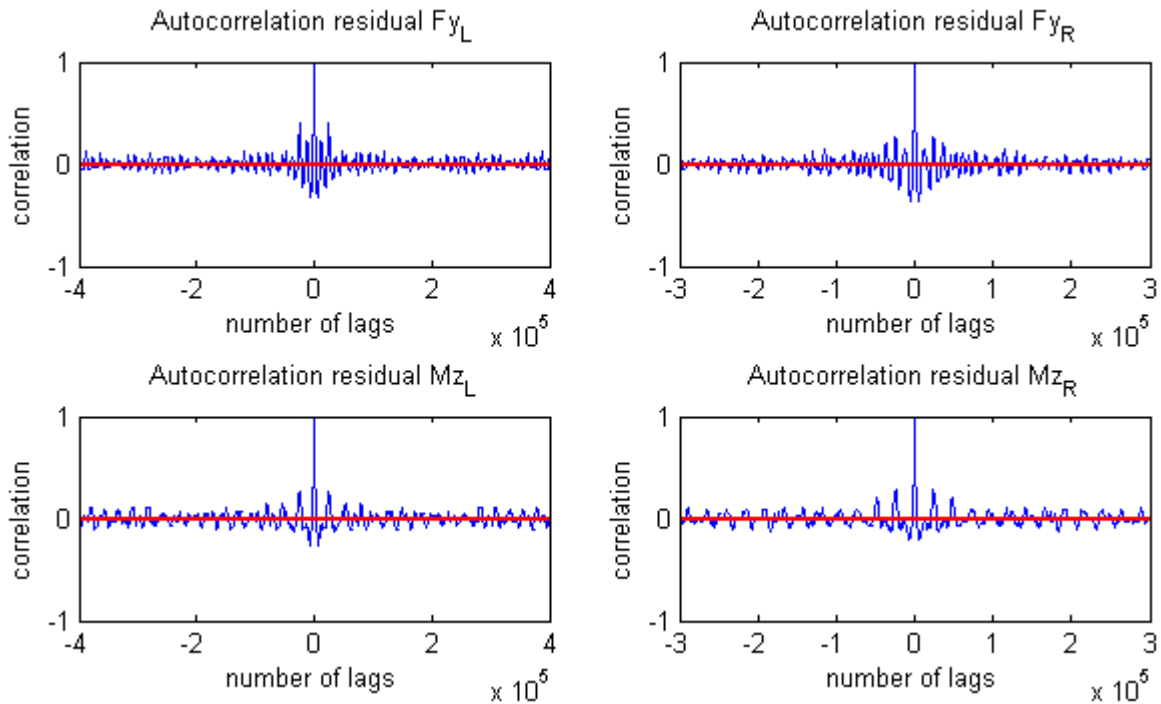
- (i) The sequence  $\hat{\epsilon}(k, \hat{\theta})$  is a zero-mean white-noise sequence.
- (ii) The sequence  $\hat{\epsilon}(k, \hat{\theta})$  is statistically independent from the input sequence  $u(k)$ .

Figure 2-19 shows the autocorrelation for the model residuals. If the first property (i) holds, the autocorrelation of the residuals should be a unit pulse. Because the amount of data is finite, 95 % confidence bounds are defined between which the autocorrelation function should be for lags unequal to zero. The confidence bounds are found as:

$$\pm 1.96 \cdot \sqrt{N}$$

With a total of  $8 \cdot 10^5$  datapoints, the confidence bounds for the model are found as  $\approx \pm 2 \cdot 10^{-3}$ . In Figure 2-19 the confidence bounds are drawn as red lines very close to the x-axis and it becomes clear that the first property does not hold for the identified model. However, this makes sense by looking at Figure 2-16 and realizing that the residual is not a zero-mean white-noise sequence. Instead, the noise is probably caused by differences in other forces, road texture, vibrations and temperature [19][20].

Figure 2-20 and Figure 2-21 show the cross-correlations between the model residuals and the inputs for the left- and right model respectively. If the second property (ii) holds, the cross-correlation should be between the confidence bounds for all lags. It is clear that this property also does not hold but this makes sense because the strain inputs are influenced again by differences in other forces, road texture, vibrations and temperature. The signals measured with the LSBs could be improved by taking these different noise contributors into account and designing a bearing specifically for load sensing. The LSB signals can be used for the haptic steering feedback experiments but the experiment has to be closely monitored and the controller should be designed taking the limitations on the quality of the load measurements into account.



**Figure 2-19:** Autocorrelation residuals strain model with VELOS measurement wheel

### Hall effect sensors

The same procedure as before can be used to identify a model using the hall effect sensors as inputs. In this case there are only two inputs instead of three, because the developed LSBs only have an hall effect sensor at the top- and at the bottom. Figure 2-11 provided an indication that the filtered hall effect signals contain information about the tire-road forces. These filtered signals are used to create a model again using a MLRA with the real measurements from the VELOS measurement wheel. Figure 2-22 shows a comparison of the identified lateral force and aligning moment hall effect model with the VELOS measurement wheel and strain model. The noise at the beginning and end of the dataset is caused by the holes in the ABS ring and the fact that the velocity dependent notch filter is cut-off at speeds below  $5 \text{ m/s}$  to prevent errors. However, for higher speeds the lateral force estimation looks good again. The

coefficients of the lateral force model are found below:

**Table 2-3:** Coefficients of LSB hall effect models

LEFT		RIGHT	
$\beta_{1,1,F_y}$	-500.3	$\beta_{1,1,F_y}$	499.9
$\beta_{1,2,F_y}$	-486.0	$\beta_{1,2,F_y}$	487.9

The signs are different and the magnitude of the numbers is approximately the same. This makes sense because a tilting movement of the ABS ring is measured and for one sensor the distance becomes smaller whereas for the other sensor the distance becomes larger.

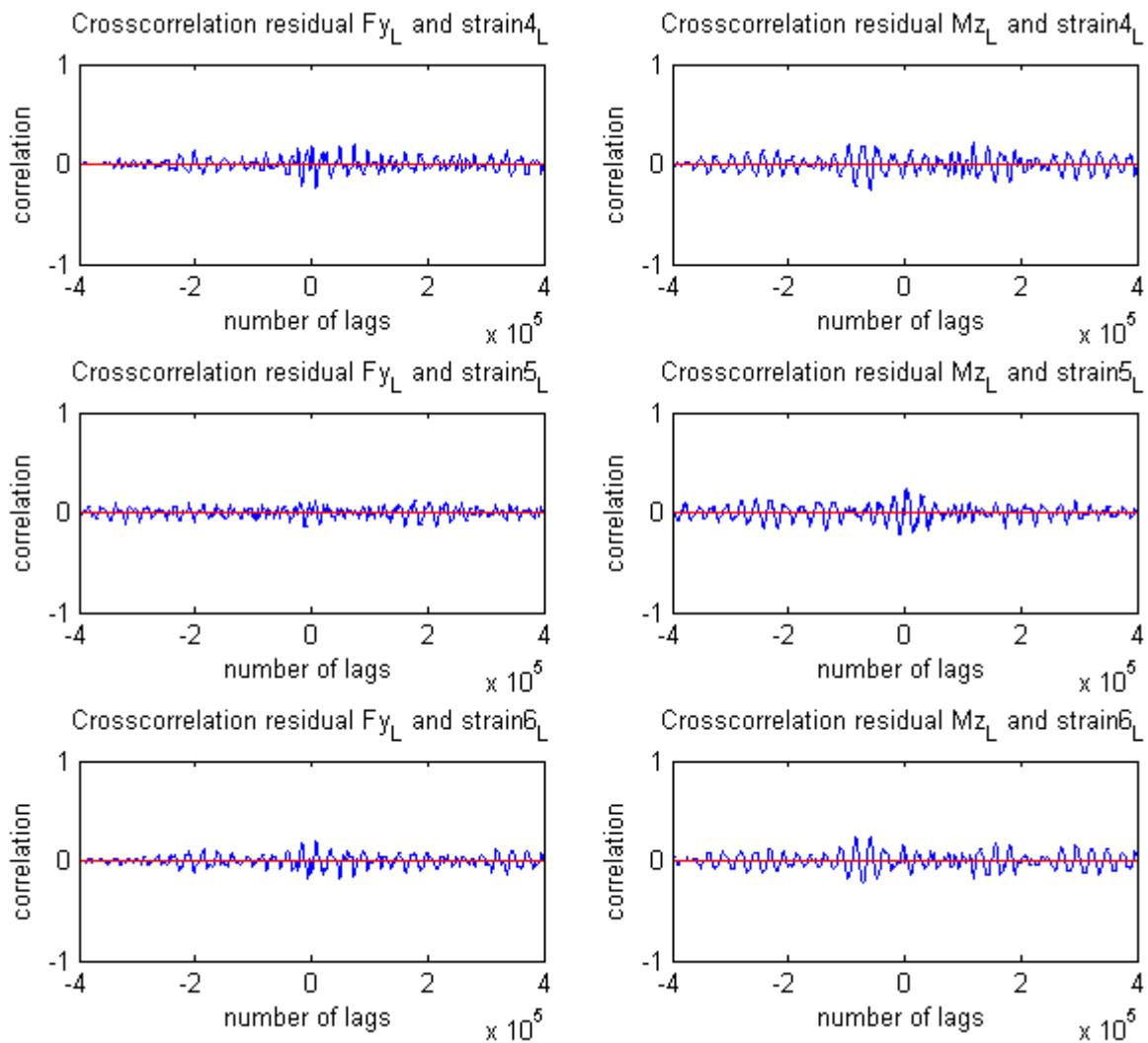


**Figure 2-20:** Cross-correlation strain inputs with residuals strain model for left front wheel

Unfortunately the aligning moment estimation is not valid at all, see Figure 2-22. This can be explained by looking at the bearing geometry and the placement of the hall effect sensors in Figure 2-1. Since the hall effect sensors are placed at the top and at the bottom on a vertical line it is of course not possible to identify a moment around the vertical axis with only these sensors. A recommendation for the future is to include at least three hall effect sensors to be able to identify the aligning moment as well. The results shown in this thesis are an indication that hall effect sensors might be a suitable alternative for strain gauges and further investigation is recommended.

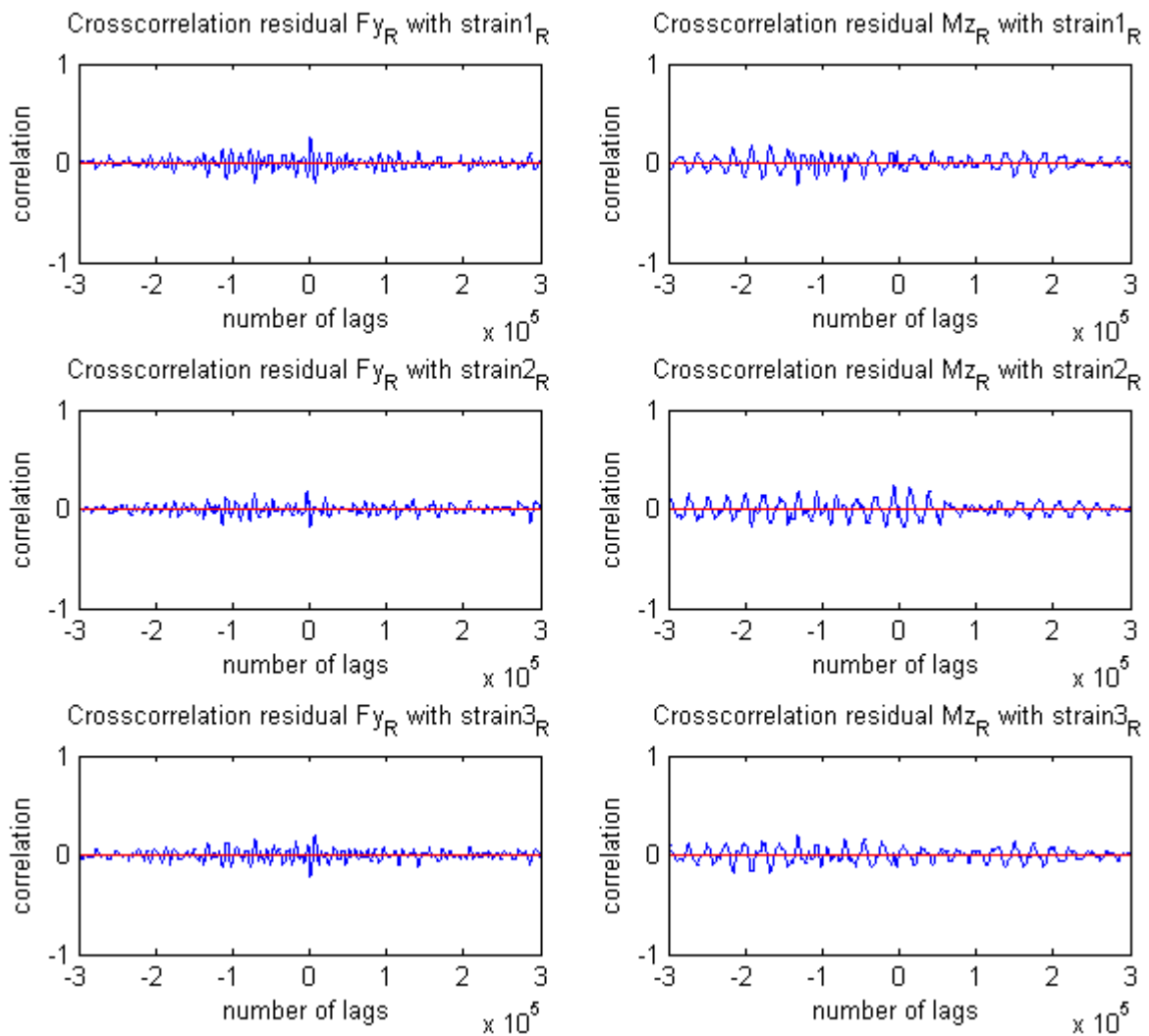


**Figure 2-21:** Cross-correlation strain inputs with residuals strain model for right front wheel

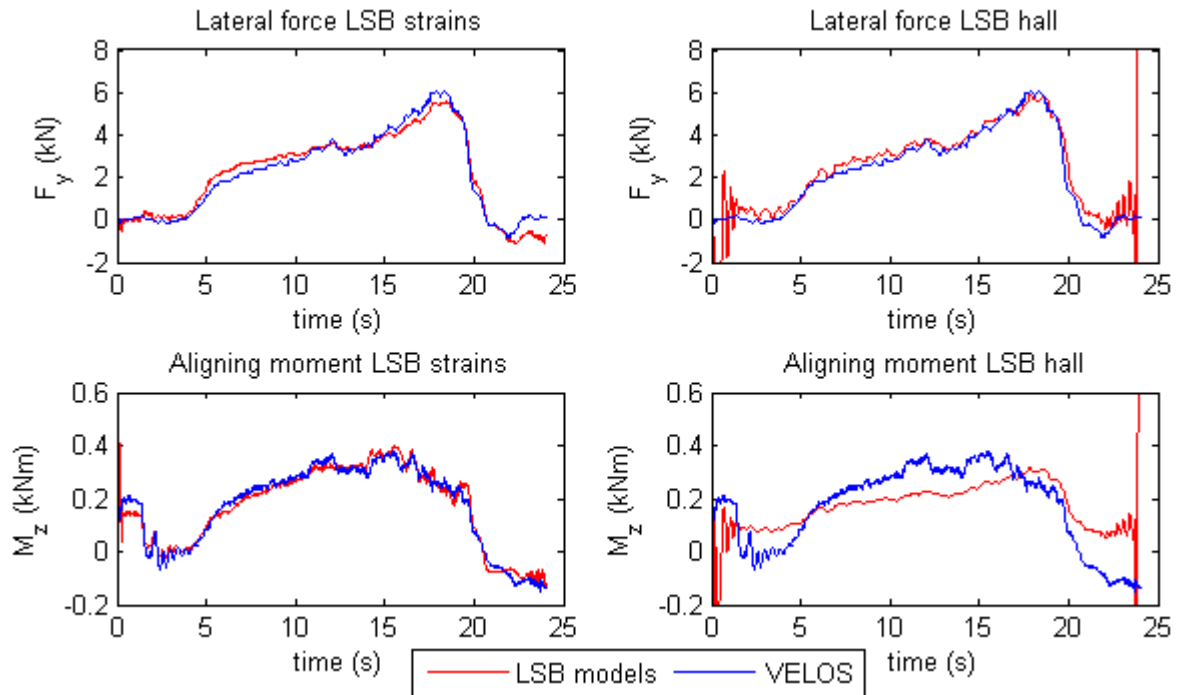


**Figure 2-22:** Lateral force and aligning moment hall effect model comparison with VELOS measurement wheel and strain model

## 2-4 Conclusion

Lateral force estimation with the strains on LSBs can yield good results for controlled experiments. However, the estimation is mainly based on load transfer during cornering and hence depends strongly on the vertical force instead of the lateral force. The estimation is also disturbed by longitudinal forces during acceleration and heavy braking. Therefore the estimation will be disturbed if the LSBs are used in more dynamic driving conditions and on roads driving over bumps. Temperature- and drift influences are a problem and a work around for the haptic feedback experiments is found in zeroing the signals every time the vehicle velocity is zero. The estimation of the aligning moment also provides good results and the drop in aligning moment is clearly visible as the tire limit is approached. However, the estimation is not as good as for the lateral force mainly because the total amplitude is much smaller.

The hall effect sensor results look promising, but since the ABS ring has holes more filtering is needed. Unfortunately the LSBs in the Opel Astra have only two hall effect sensors placed in a vertical line which makes estimation of the aligning moment impossible. The results for the lateral force estimation are an indication that hall effect sensors might be a suitable alternative for strain gauges and further investigation is recommended.

Figure 2-23 provides a general overview of important vehicle states and driver inputs. A drop in aligning moment is clearly visible between 15 and 20 seconds. The increased velocity

while the steering wheel angle and yaw-rate remain nearly constant and the large front axle slip angle compared to rear axle slip angle verify that this is indeed an understeer situation. The estimations of the lateral force and aligning moment based on the strain gauges are used for the haptic steering feedback experiments described in the next chapter.

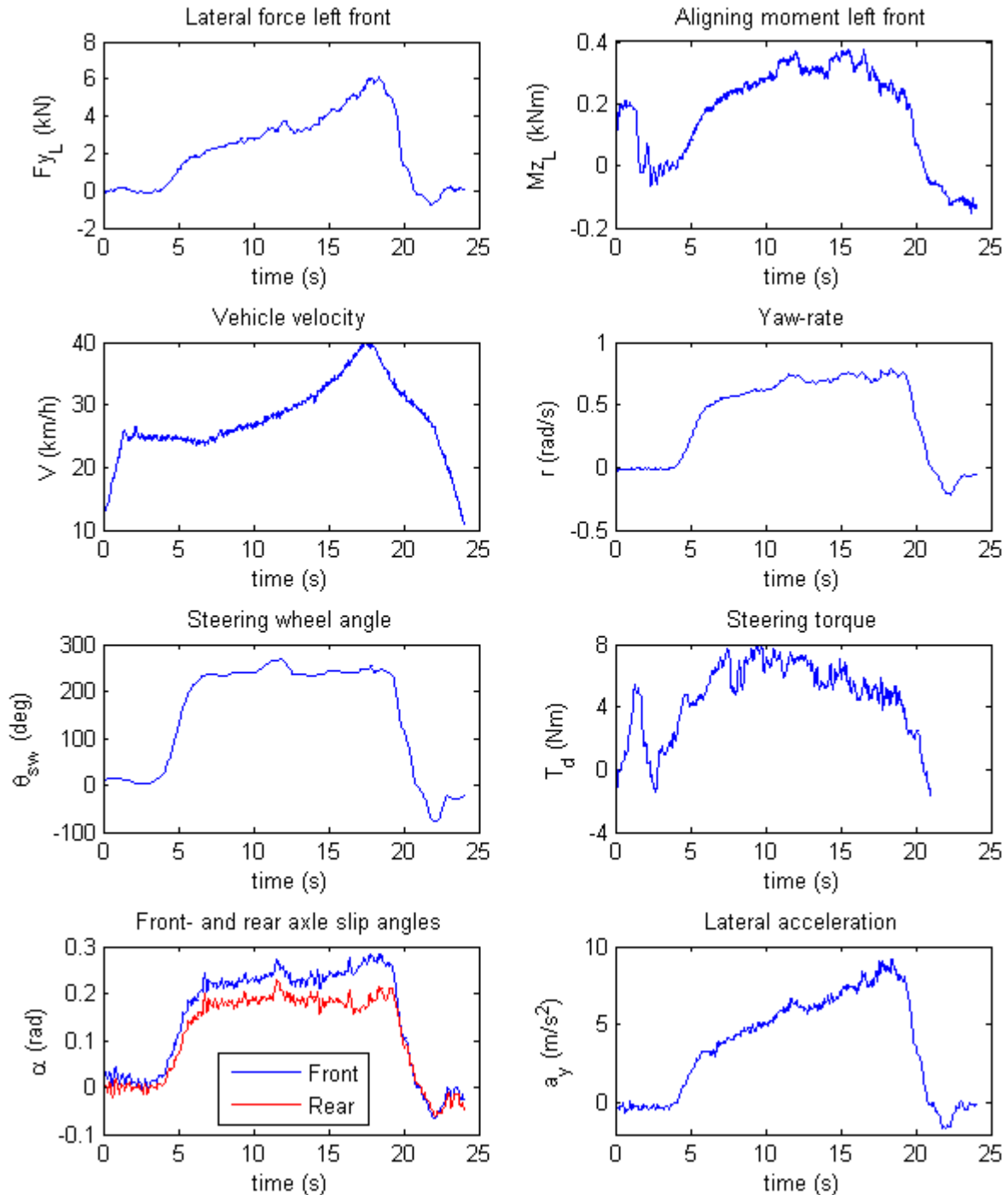


**Figure 2-23:** Vehicle states and driver inputs clockwise circle measured with Opel Astra

# Haptic feedback

### 3-1 Description

#### 3-1-1 General

The Haptic Support Near the Limits (HSNL) system [4] was developed using a model based approach combining slip angle measurements with a tire model to amplify the drop in aligning moment on the steering wheel. In this chapter a direct wheel load measurement approach is applied using measurements of the lateral force and aligning moment with Load Sensing Bearings (LSBs). Looking at Figure 1-1 the ratio of lateral force to aligning moment increases as a vehicle is closer to the limit and this can be used to generate the haptic feedback signal for the electric motor on the steering wheel. Unfortunately the ratio also depends on the vertical force. Reason for this is that as the vertical force changes, the aligning moment decreases relatively more than the lateral force since the lateral force as well as the pneumatic trail depend on vertical force [11][8]. Load transfer changes the vertical forces as the lateral force changes. This means that the haptic feedback can not be made independent from road surface by looking at the ratio of lateral force to aligning moment alone. More research would be needed on the relations between different forces and moments and the tire contact patch deformation which defines the pneumatic trail. However, the haptic feedback experiments with test subjects will all be conducted on the low  $\mu$  circular surface seen in Figure 2-5 and the haptic feedback controller used in this thesis will be tuned for this specific road surface.

#### 3-1-2 Model

Appendix C shows a detailed Simulink model used to generate the signal for the haptic feedback electric motor on the steering wheel. The inputs of the model are the steering torque and the lateral force and aligning moment identified with the strain gauge measurements from the LSBs and the output is a signal for the haptic feedback electric motor on the steering wheel. The tuning parameters are  $Mz\_plus$  or  $c$ ,  $sat_L$  and  $sat_R$ ,  $offset_L$  and  $offset_R$  and  $T\_driver\_gain$ . The influence of the different parameters and tuning of the feedback signal

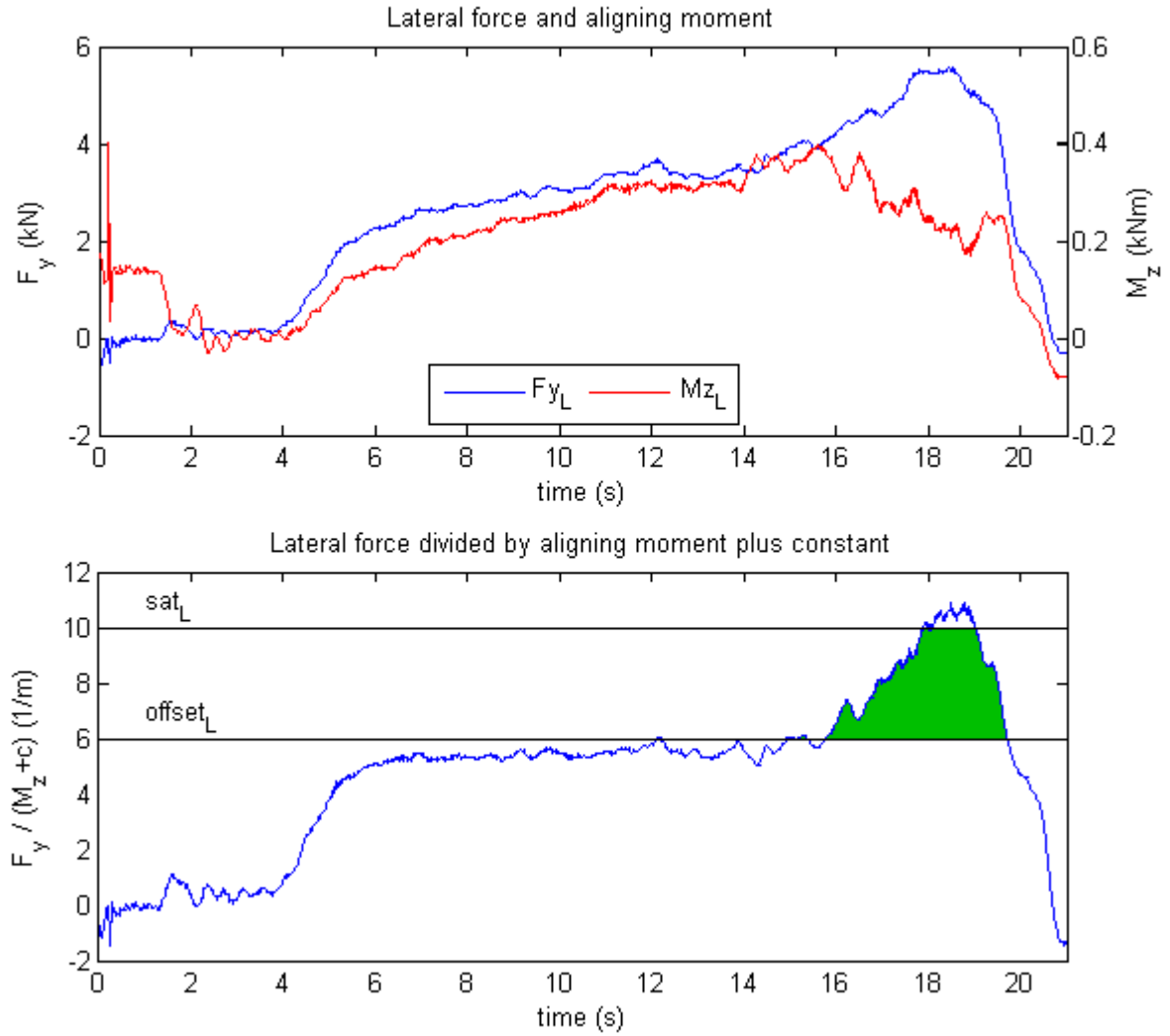


**Figure 3-1:** Tuning of parameters haptic feedback controller

is described below. The haptic feedback signal is calculated based on load measurements from the outside wheel during cornering. The upper plot in Figure 3-1 shows the lateral force and the aligning moment as identified for the left front wheel for one of the datasets driving a clockwise circle towards the limit. The lower plot shows the ratio of lateral force to aligning moment. The constant term  $c$  or  $Mz\_plus = 0.3$  (see Appendix C) is added to the measurements of the aligning moment  $M_z$  in the ratio calculation to make sure the ratio is robust to disturbances especially if  $F_y$  and  $M_z$  are close to zero. If this constant term is not used, then the ratio  $\frac{F_y}{M_z}$  is heavily fluctuating between plus and minus infinity for measurements of  $F_y$  and  $M_z$  close to zero. If the constant is made very large then the ratio  $\frac{F_y}{M_z + c}$  is almost proportional to the lateral force and the aligning moment has no influence. A lower limit for the haptic feedback signal is defined by the tuning parameter  $offset_L$ . If the ratio  $\frac{F_y}{M_z + c}$  is lower than or equal to this value then the normalized haptic feedback signal is equal to zero which means the haptic feedback electric motor is not active. An upper limit



for the haptic feedback signal is defined by the tuning parameter  $sat_L$ . If the ratio  $\frac{F_y}{M_z + c}$  is equal to or larger than this value then the normalized haptic feedback signal is equal to one. Between the lower limit  $offset_L$  and the upper limit  $sat_L$  the haptic feedback signal is scaled between zero and one. The haptic feedback system is active between 16 and 20

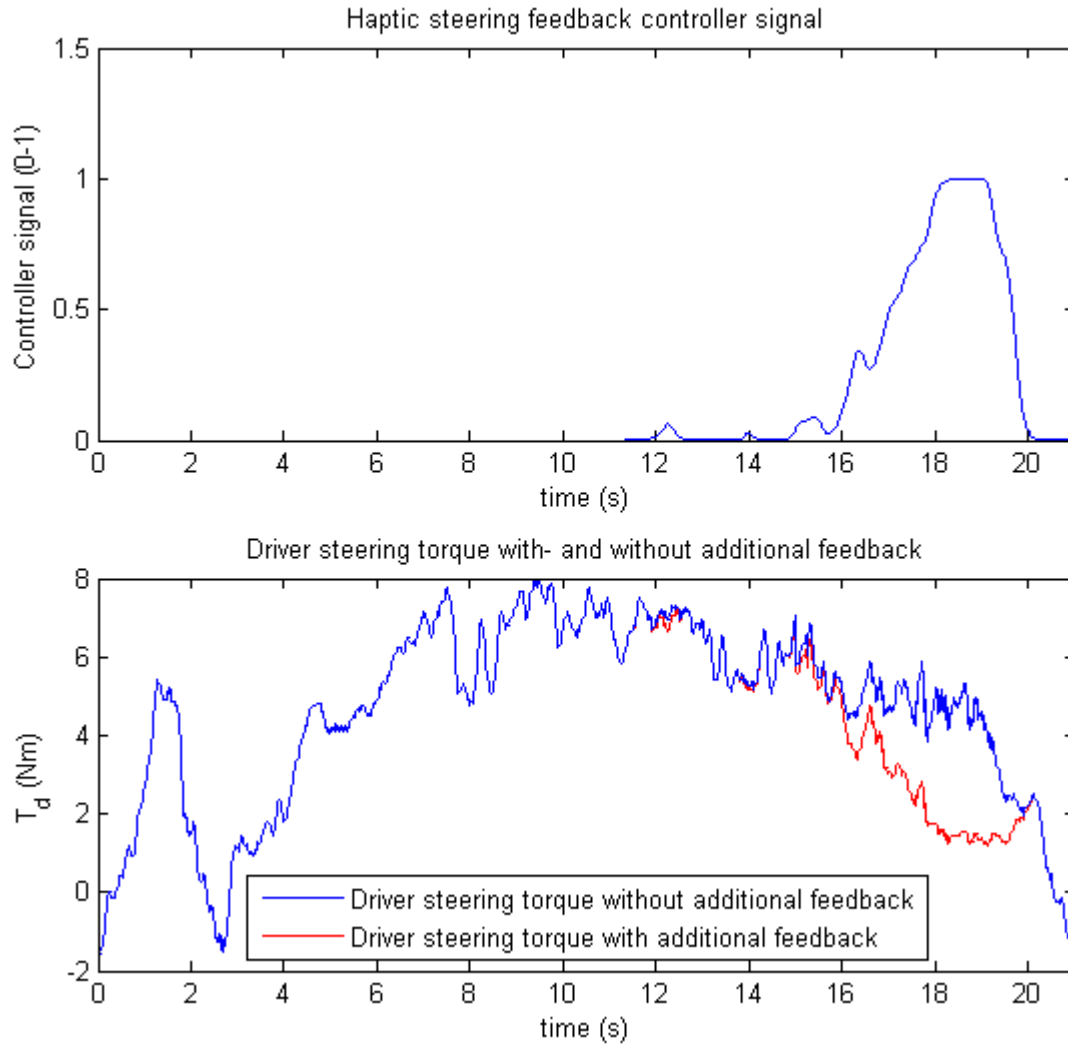


**Figure 3-2:** Haptic feedback controller signal and driver steering torque

seconds defined by the green area in Figure 3-1. The feedback signal obtained by scaling the green area in Figure 3-1 between zero and one can be found in the upper plot in Figure 3-2. The normalized signal is multiplied with the filtered driver torque and the tuning parameter  $T\_driver\_gain = 0.7$ . The result is a haptic feedback signal for the electric motor in  $Nm$  which can be between zero and 0.7 times the driver torque. This means the total steering torque will always remain self-aligning. The lower plot shows the driver torque with- and without additional feedback on the steering wheel. It is clear that between 16 and 20 seconds the steering torque is reduced by the additional feedback which should warn the driver that he is driving close to the limit. The simulink model creates the haptic feedback controller

signal for the electric motor on the steering wheel with the mathematical description given below.  $C$  is the haptic feedback controller signal normalized between zero and one and from this equation it becomes clear that the maximum reduction in steering torque by the electric motor is equal to 70 %.

$$C = \max \left( \frac{\min \left( \max \left( \frac{F_{Y,L}}{\max((M_{Z,L} + c), 0.001)}, 0 \right), sat_L \right)}{sat_L} \cdot \frac{sat_L + offset_L}{sat_L} - \frac{offset_L}{sat_L}, 0 \right)$$

$$T_m = C \cdot 0.7 \cdot T_d$$

## 3-2 Experiments

### 3-2-1 Goal

The goal for the haptic feedback experiments is to show that an amplification of the drop in aligning moment can be beneficial for the driver. The system should increase safety by making it easier for the driver to keep control of the vehicle and prevent inputs leading to terminal understeer. Because the driver is kept in-the-loop and has a better understanding of what the vehicle is doing this has the potential of increasing driving pleasure and comfort. Improvements can be evaluated in two different ways: with an objective and a subjective method. The objective method consists of looking at differences in vehicle states and driver inputs with and without active feedback system. The subjective method checks the drivers own experience during driving with- and without active feedback system. This is evaluated using the evaluation form found in Appendix D.

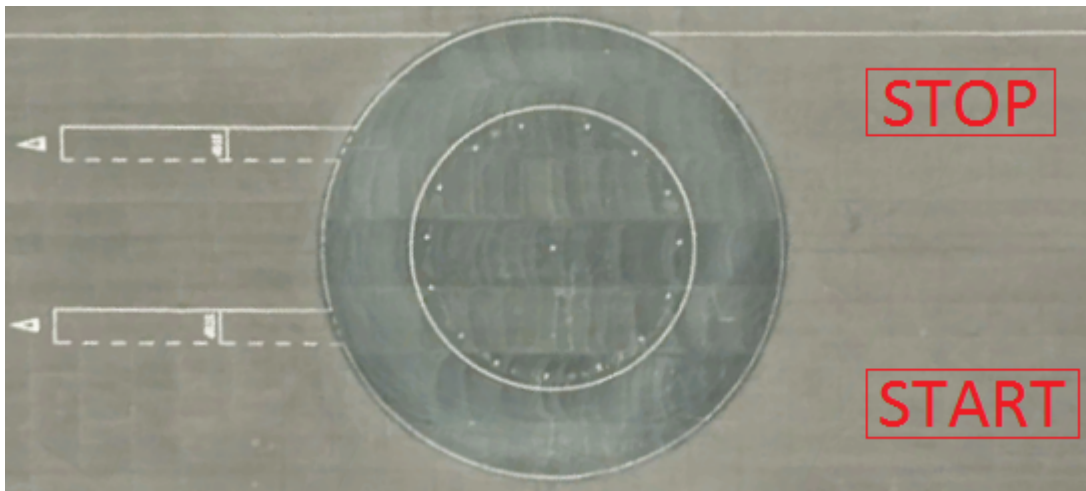


**Figure 3-3:** Top view of the low  $\mu$  circular surface at the Prodrive test track [21]

### 3-2-2 Testing procedure

The experiment with test subjects is conducted on 27-03-2014 at the Prodrive test track on the low  $\mu$  circular surface ( $\mu = 0.25 - 0.3$ ) made wet with sprinklers, see Figure 2-5. 16

people were invited to take part in the experiment and 13 people accepted the invitation. The 13 people were divided in four groups divided over the day in sessions of two hours. For each group the sessions started with an explanation of the research project, the haptic feedback system on the steering wheel, the testing procedure and the evaluation form. All people got to do two runs, one with- and one without the feedback system switched on. Seven people did their first run without feedback and their second run with feedback and six people did it the other way around. This should account for the learning effect that people have when performing a specific maneuver multiple times. Test subjects are not told if they are driving with additional feedback or not.

A run is started as follows: the driver is instructed to drive to the start position marked with four cones, facing towards the circle, see Figure 3-3. The instructor (the author of this thesis) is sitting next to the driver in the passenger seat and controls the switch for the feedback system and data acquisition system. The data acquisition and if necessary the feedback system is started and the driver is instructed to drive clockwise circles over the slippery surface in second gear while keeping the inner wheel on the inside white line. In case of a complete spin or after five completed laps the driver is instructed to bring the vehicle to standstill in the stop area. The instructor stops the data acquisition and the feedback system and the driver is instructed to drive the vehicle to the start area again. The maneuver is performed three times in total and this concludes the first run. For the second and third times performing the maneuver the drivers are instructed to set the fastest lap time while keeping the vehicle with the inner wheel on the inside white line. If the driver has performed the maneuver three times this concludes the first run. The driver is asked to fill in the front side of the evaluation form and the next driver can take place in the vehicle to start the experiment. If all drivers in one session have done their first run they all get to do their second run with opposite feedback setting compared to their first run. After the drivers have performed their second run they are asked to fill in the back side of the evaluation form.

### 3-2-3 Evaluation form

The used evaluation form can be found in Appendix D. The front side of the evaluation form starts with personal details and some questions to determine the driving experience of the test subject. This is used to get an idea of the average driving experience of the test group. It could also help in the evaluation to discard data if one of the test subjects has a lot more or a lot less experience than all the others. The second part of the front side of the evaluation form consists of the Task Load Index (TLX) developed by National Aeronautics and Space Administration (NASA). In this TLX the test subject is asked to grade mental demand, physical demand, temporal demand, performance, effort and frustration on a scale with 21 points. After the second run the back side of the evaluation form has to be filled in which starts again with the TLX. The second part of the back side consists of some questions to check if drivers felt the difference between the two runs and if they liked the first or second run better in terms of comfort, safety, performance, pleasure and perceived grip level. At the end of the evaluation form some space is available to leave general comments about the experiment.

### 3-3 Results

#### 3-3-1 Data processing

Each of the 13 test subjects performed the five lap maneuver three times with and three times without feedback. This should result in a total of 78 datasets, but not all datasets are selected for the analysis since a few datasets are corrupt and in some cases the system was not working correctly. If one of the datasets with- or without feedback is corrupted the dataset with opposite feedback setting is also not used for this test subject to be able to evaluate the results using a paired t-test. 52 datasets are used for the analysis, 26 with- and 26 without haptic feedback on the steering wheel. The total length of the used data is 3868 seconds which means the average time for performing the maneuver is 74 seconds.

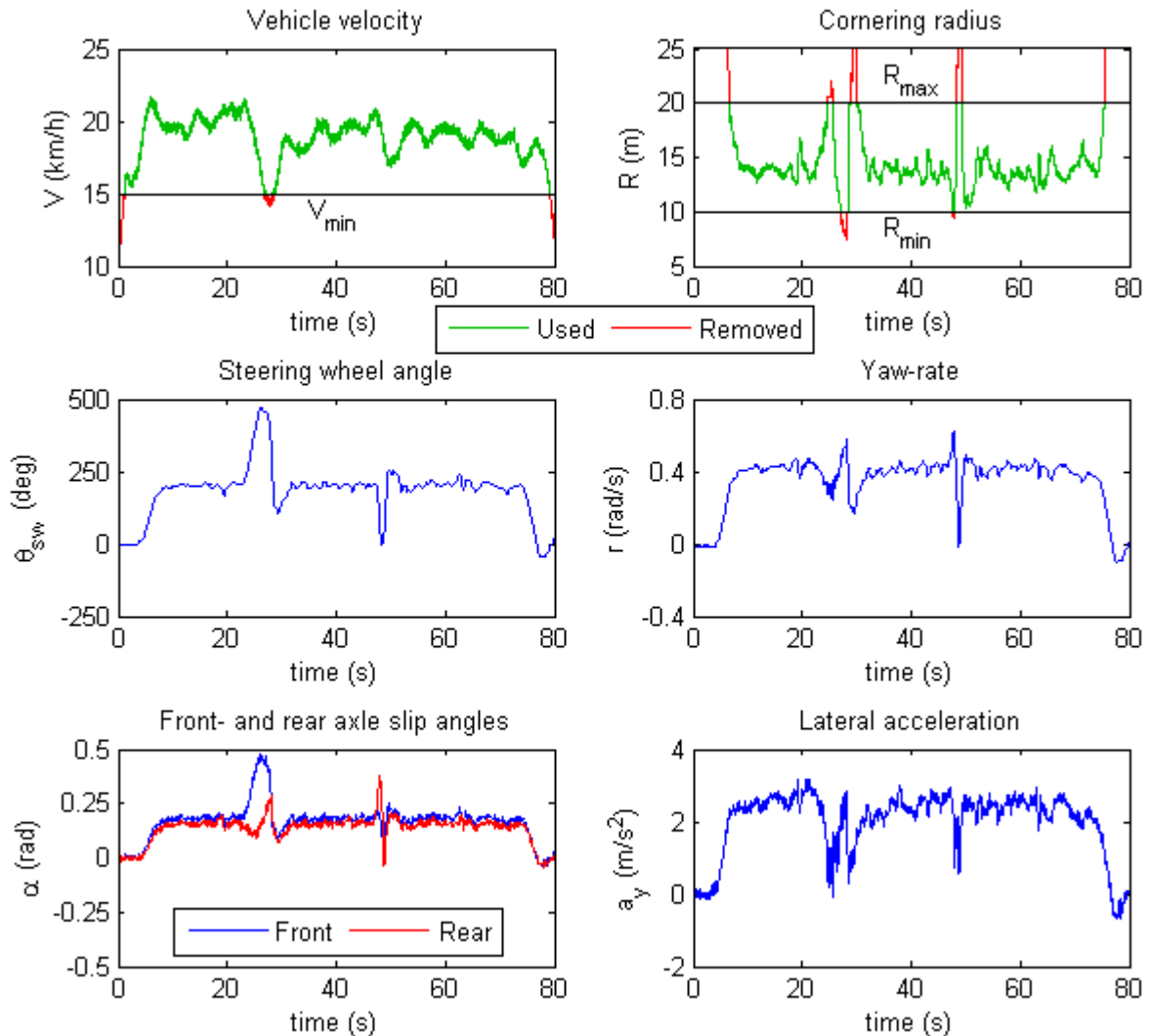


**Figure 3-4:** Example dataset with understeer situation (begin) and oversteer situation (end) to show data to be removed from the analysis based on velocity and cornering radius

The first and last five seconds of each dataset are excluded from the analysis to remove data from starting and stopping the maneuver and the vehicle speed has to be at least 15 km/h for the data to be used in the analysis. All data for which the vehicle is making a cornering radius of less than 10 m or more than 20 m are defined as loss of control or recovering from loss of control and this data is also removed from the analysis, see Figure 3-4. For every dataset the Root Mean Square (RMS) value and variance is calculated for different vehicle states and driver inputs which results in 52 RMS values and variances. A paired t-test is performed on these RMS values and variances resulting in p-values for every evaluated vehicle state or driver input. This determines if the null hypothesis that the values with- and without haptic feedback come from the same normal distribution is supported or rejected with some statistical significance. If the p-value is below 0.05 the result is said to be statistically significant and the difference is assumed to be relevant. The results are shown in box plots with the median represented by a red line and the mean represented by a blue cross. The NASA TLX results are transformed from a scale with zero to 21 points to a scale with zero to 100 percent.

### 3-3-2 Vehicle states

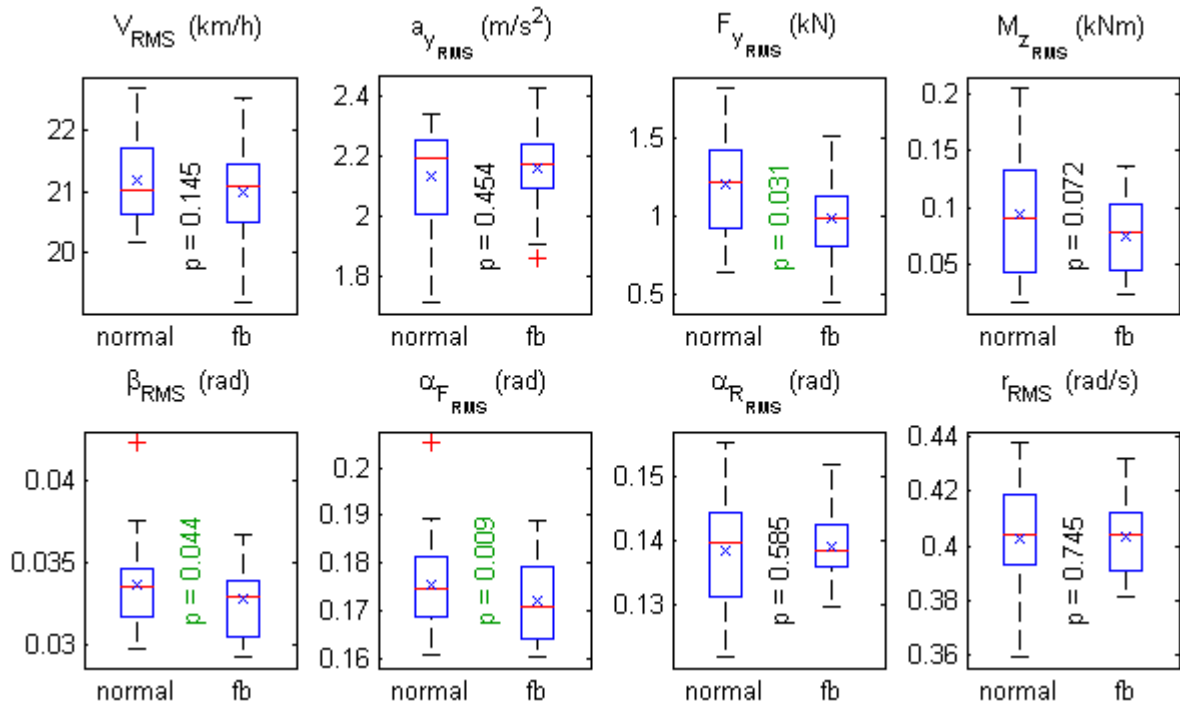
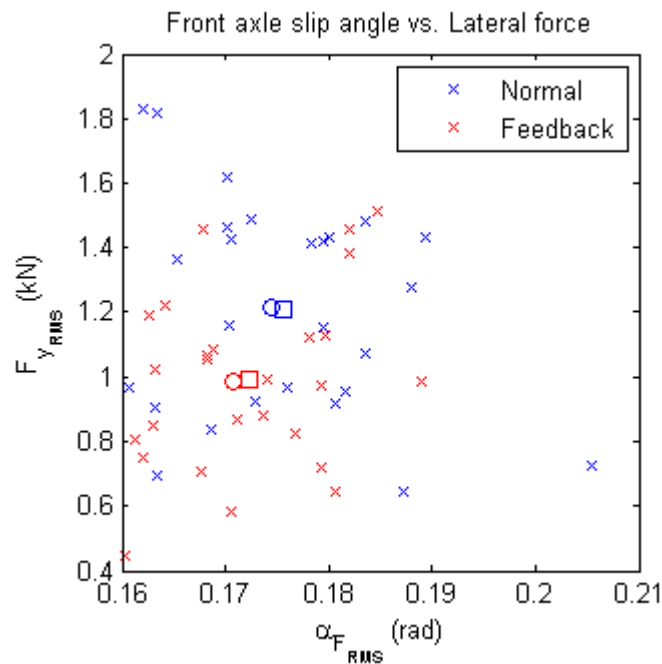


Figure 3-5: Boxplot RMS values vehicle states with and without haptic feedback

Figure 3-5 shows a boxplot of the RMS values for different vehicle states with- and without haptic feedback. The p-values for left front wheel lateral force ( $F_y$ ) and front axle slip angle ( $\alpha_F$ ) are below 0.05 indicating that these differences are relevant. The front wheel lateral force is lower with feedback indicating that drivers are indeed better capable of preventing inputs leading to terminal understeer. The front axle slip angle is also lower with feedback but the difference is smaller here. Figure 3-6 shows the RMS values of the front axle slip

angle vs. left front wheel lateral force. The mean and median are plotted with a circle and square and are both closer to the origin for the system with feedback. If this is compared to Figure 1-1 the conclusion is that indeed drivers stay further away from the nonlinear region of the tire curve with additional feedback on the steering wheel. The p-value for the vehicle slip angle ( $\beta$ ) is also below 0.05 and the vehicle slip angle is lower with feedback compared to the normal situation. A lower rear axle slip angle is also expected but not found in the evaluation



**Figure 3-6:** Plot front axle slip angle vs. lateral force RMS values with and without haptic feedback, each cross represents one run. circle (mean) square (median).

of the results. This might be explained by the fact that the haptic feedback system is only based on load measurements of the front wheels. If the rear tires lose grip before the front tires do, the test subject does not feel this in the haptic feedback on the steering wheel. The vehicle might already be getting into an oversteer state but the driver is slower in correcting this than for an understeer situation because the haptic feedback on the steering wheel does not provide a warning. It is interesting to repeat the experiment with LSBs in the rear wheels and an extended haptic feedback system which also provides a warning for the driver if the rear tires are close to the limit. This is recommended for future work. The driver is preventing the front tires from saturating resulting in lower lateral force and lower front axle slip angle but there is not really a difference in cornering radius, see Figure 3-7. The test subjects were given the task to keep the inner wheel on the inside white line of the circle and set the fastest time. The goal was that the test subjects would prevent saturation of the front tires. This should prevent the vehicle from sliding off the circle and should result in a smaller cornering radius. Test subjects actually managed to prevent saturation of the front tires better, but this did not lead to a statistically significant decrease in cornering radius. It would be interesting to repeat the experiment for example with cones or other obstacles to mark the outside boundaries of the desired path. Both with- and without additional feedback

the number of loss of control incidents is equal to 26 which is an average of one per run. Although drivers are better capable of preventing saturation of the front tires this does not automatically mean that the system increases safety.

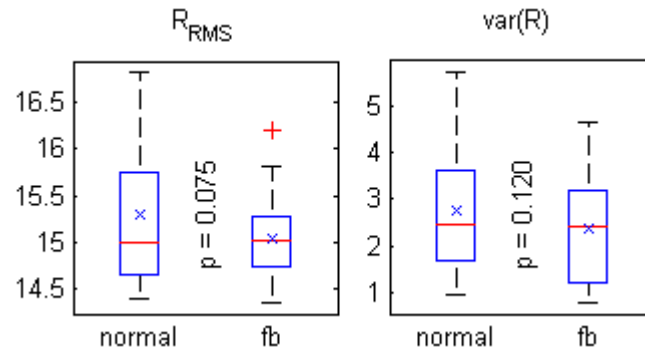


**Figure 3-7:** Boxplot RMS values and variances cornering radius with and without haptic feedback

The boxplot with variances for different vehicle states is displayed in Figure 3-8. Since all p-values are above 0.05 no relevant differences are found. However, the variances of the lateral force and aligning moment are lower with feedback and the p-values are still small. This is an indication that test subjects are better capable of keeping the vehicle in a steady-state condition around the grip level that they perceive as maximum, see Figure 1-1.

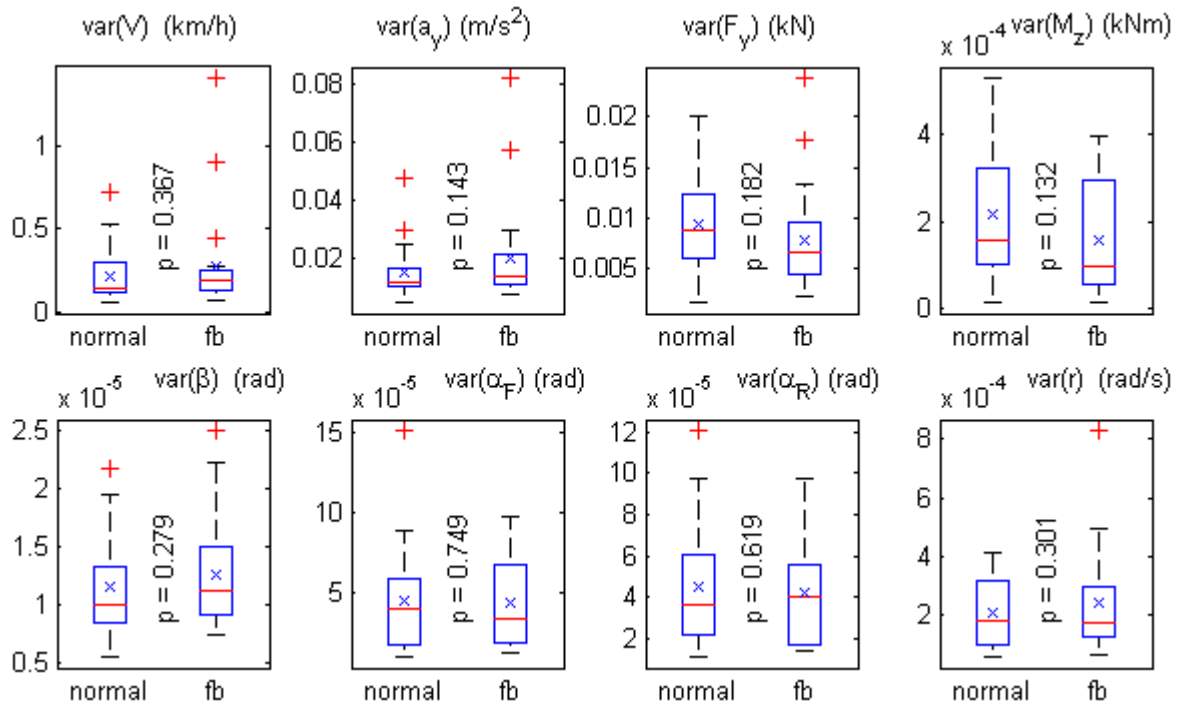


**Figure 3-8:** Boxplot variances vehicle states with and without haptic feedback

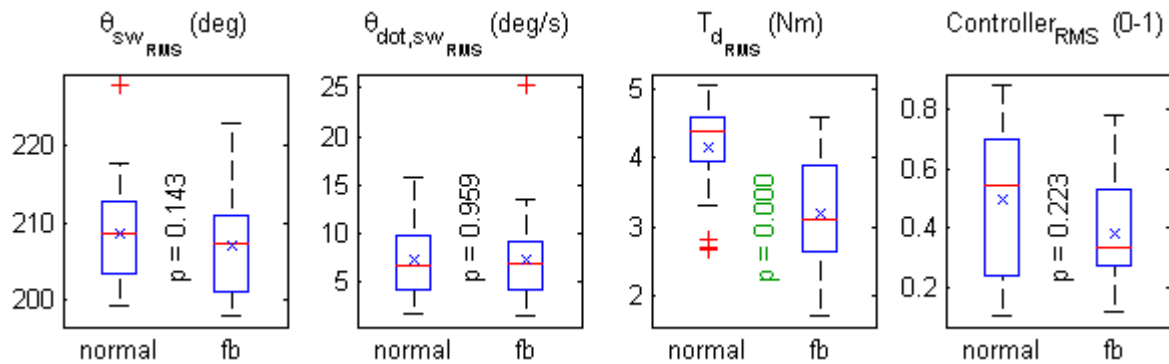


**Figure 3-9:** Boxplot RMS values driver inputs and controller signal with and without haptic feedback

Figure 3-9 shows the RMS values for steering wheel angle, steering wheel speed, steering torque and haptic steering controller signal. Of course the haptic feedback controller was not active for the normal case but this plot shows what the system would have done if it was active. A relevant difference is found for steering torque with a p-value below 0.001. The steering torque is much lower with feedback which makes sense since this is exactly what the feedback system does: decreasing the steering torque as the front tires approach the limit. The variances of steering wheel angle, steering wheel speed, steering torque and haptic steering controller signal shown in Figure 3-10 show no relevant differences.

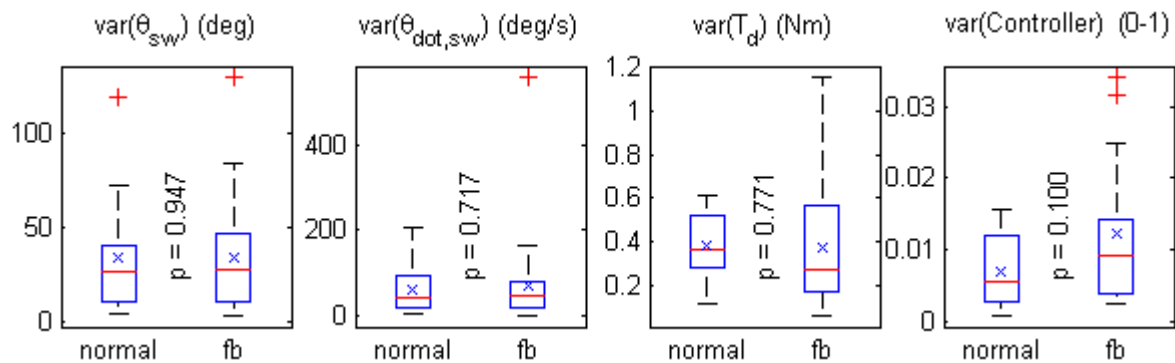


**Figure 3-10:** Boxplot variances driver inputs and controller signal with and without haptic feedback

A different way of looking at the driver steering input is by looking at the Steering wheel Reversal Rate (SRR) [22]. This is defined as the number of clockwise to counterclockwise changes in steering direction in one minute. Clockwise to counterclockwise steering reversals are only counted if the steering wheel speed is higher than  $3 \text{ deg/s}$ . The SRR can be seen as a measure of control effort. Figure 3-11 shows a relevant difference  $p = 0.041$  and the SRR is lower with feedback system. This means the control effort for the driver is lower with feedback system which can potentially increase safety, driving pleasure and comfort. However, note that the distribution is not normal but it is skewed to the right. This means that the t-test which is based on the mean is influenced much more by the largest values and hence it is not very robust. In this case it is better to use the signed rank test which tests if the samples



in the two datasets come from a distribution with equal median. This p-value is also given in Figure 3-11 and does not show a relevant difference for the SRR with- and without haptic feedback. Instead of using the datasets of the maneuvers separately, another way to do the

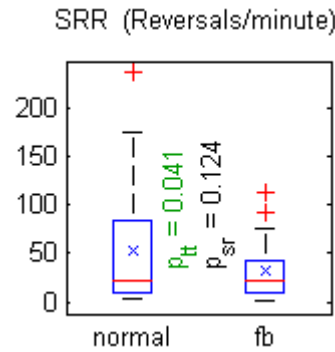


**Figure 3-11:** Boxplot Steering wheel Reversal Rate (SRR) with and without haptic feedback

analysis can be to first combine the datasets for each test person. This means that instead of  $2 \times 26$  RMS values now  $2 \times 13$  RMS values are used for the analysis. Table 3-1 shows the p-values for this method. The results for lateral force and driver torque are still statistically significant and the lower RMS value of the controller is now statistically significant as well. However, although the p-values for vehicle slip angle and front axle slip angle are still low, they are not below 0.05 anymore.

**Table 3-1:** Important values analysis  $2 \times 26$  separate datasets and  $2 \times 13$  datasets by test subject

	By dataset ( $2 \times 26$ total)			By test subject ( $2 \times 13$ total)		
	mean (normal)	mean (fb)	p-value	mean (normal)	mean (fb)	p-value
$F_{Y_{RMS}} (kN)$	1.207	0.990	0.031	1.239	0.999	0.043
$\beta_{RMS} (rad)$	0.034	0.033	0.044	0.034	0.033	0.183
$\alpha_{F_{RMS}} (rad)$	0.176	0.172	0.009	0.177	0.173	0.079
$T_{d_{RMS}} (Nm)$	4.150	3.188	0.000	4.230	3.261	0.014
$Controller_{RMS} (0-1)$	0.497	0.383	0.223	0.552	0.288	0.011
$SRR (Rev/min)_{tt}$	53.330	31.336	0.041	60.797	34.103	0.159
	median (normal)	median (fb)	p-value	median (normal)	median (fb)	p-value
$SRR (Rev/min)_{sr}$	22.744	22.125	0.124	42.990	27.041	0.492

### 3-3-3 Evaluation form

The experiment was conducted with 13 test subjects. Their characteristics obtained from the first part of the evaluation form can be found in Table 3-2. All test subjects are male and they are on average 40.7 years old. 10 of the 13 test subjects filled in that they have professional driving experience, examples are: advanced driving courses, evaluation- and test drives and slip courses. The test subjects own their driving license 23.3 years on average and have owned

more than 11 cars on average. Only two of the test subjects have not experienced a crash on the public road and the average number of crashes for the test subjects is 2.1. They grade their driving skill 7.2 on average. These characteristics are an indication that the test group consists of a more than average number of car enthusiasts. This might influence the results, and experiments with more test subjects would be needed to generalize the conclusions for average drivers.

**Table 3-2:** Driver characteristics 13 test subjects

	Sex	Age	Professional driving experience	Years owning license	Cars owned	Crashes public road	Grading driving skills
1	male	28	yes	11	8	1	10
2	male	41	yes	24	13	2	6
3	male	33	yes	16	6	2	7
4	male	36	yes	18	8	3	7
5	male	44	no	25	10	0	8
6	male	41	yes	23	20+	0	7
7	male	44	yes	27	11	10	7
8	male	40	yes	23	15	2	7
9	male	49	yes	32	10	1	8
10	male	54	yes	36	15	3	7
11	male	40	no	23	10	1	6
12	male	42	no	25	9	1	6
13	male	37	yes	20	10	1	8
Sum	-	529	-	303	145+	27	94
Average	-	40.7	-	23.3	11+	2.1	7.2

The results of the NASA TLX can be found in Figure 3-12. Although the mental demand, physical demand, effort and frustration seem to be lower for the feedback system none of the results has a p-value below 0.05 which means no conclusions can be drawn from this data. The HSNL study [4] showed relevant differences for the TLX results but in this case 25 and 17 test subjects were used for simulator and real car testing respectively and drivers got to do more runs. If the experiment in this thesis would be repeated with more test subjects and more runs for each test subject this might lead to relevant differences between the different workload aspects on the evaluation form. Another reason why the p-values might not be very low is because drivers liked their second run better than the first run. This is caused by a learning effect: they got better used to the vehicle, the road surface and the maneuver. The second part of the back side of the evaluation form showed this very clearly. Although the order of driving with- or without feedback was randomized, almost all drivers liked their second run better in terms of comfort, safety, performance, pleasure and perceived grip level. Interesting observation is that the experiment seemed to be more clear for drivers first driving without feedback and then driving with feedback than it was for drivers doing it the other way around. A possible explanation could be that test subjects are focussing on a lot of things in the first run because they have to get used to the vehicle, road surface and the maneuver and they are not really aware of the feedback. If they start their second run they try to focus on the feedback but they do not really feel anything through the steering wheel.

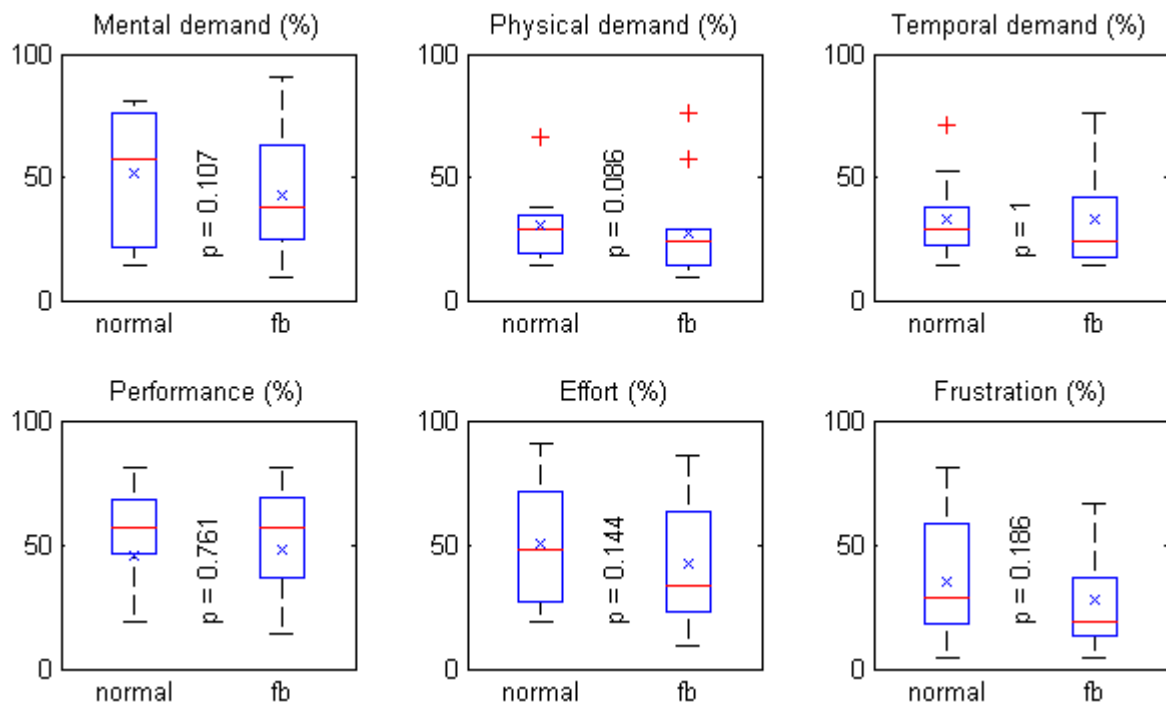


**Figure 3-12:** Boxplot evaluation form results with and without haptic feedback

Although the individual p-values for the evaluation form are not below 0.05, the mental demand, physical demand, temporal demand, effort and frustration seem to be lower for the feedback system. Since they are rated on the same scale and the expectation is that they are all lower for the feedback system, they can be lumped together in one combined boxplot. Figure 3-13 shows this boxplot of the combined evaluation form results for mental demand, physical demand, temporal demand, effort and frustration. The combined value is 14 % lower for the feedback system and now the p-value is just below 0.05.

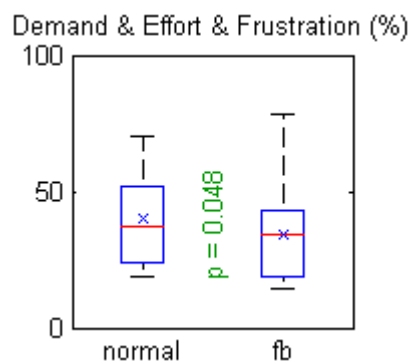


**Figure 3-13:** Boxplot combined evaluation form results demand, effort and frustration with and without haptic feedback

The general comments are used for evaluating the experience of the test subjects with the system. The comments are very far apart in some cases and again from the general comments it seems like the experiment was more clear for drivers driving without feedback in their first run and with feedback in their second run. Positive comments generally include something like: improvement in perceived grip level and improvement in feedback through the steering wheel. Two drivers reported a shift in vehicle balance between over- and understeer between the two runs. This is a very useful comment since it supports the observation that drivers were able to prevent saturation of the front tires better with feedback system but there was no warning to prevent saturation of the rear tires. Of course there are also negative comments. Multiple people were confused and felt the feedback was too weak to tell which run they had driven with feedback. Other people reported that the feedback was a bit artificial and too high for their taste. For most people the second run felt better, more natural, more intuitive or more successful but they reported this was more due to familiarity with the vehicle and the road surface rather than the change in haptic feedback.

### 3-4 Conclusion

As a vehicle approaches the limit the aligning moment drops while the lateral force is still increasing or saturates. A method to estimate how close a vehicle is to the limit is looking at the ratio of lateral force to aligning moment. Close to the limit this ratio increases and this can be used to create a normalized haptic feedback signal. To make the system more robust especially if  $F_y$  and  $M_z$  are close to zero, a constant is added to the measurements of  $M_z$ . The normalized signal is multiplied with 0.7 times the driver steering torque to make sure the feedback is weaker than the driver torque and steering does not become unstable.

An experiment was done with 13 test subjects on the low  $\mu$  circular surface at the Pro-drive test track. The results show relevant differences in vehicle states between the situation with- and without additional haptic feedback on the steering wheel. The lateral force is found to be 18 % lower with additional haptic feedback. The front axle slip angle is also found to be a bit lower but no relevant differences are found for the rear axle slip angle. This might be explained by the fact that the haptic feedback system is only based on load measurements of the front wheels and hence does not warn drivers in an oversteer situation. No difference is found for the number of loss of control incidents and no relevant differences are found for vehicle speed, lateral acceleration, yaw-rate and cornering radius. The result supports the hypothesis that the system might help to increase safety because drivers can prevent saturation of the front tires. However, more research is needed to investigate if drivers will decrease the cornering radius when driving on a normal road. It is recommended to repeat the experiments with LSBs at the rear so the haptic feedback can also warn drivers in an oversteer situation.

The mean SRR is found to be almost 50 % lower with feedback but the distribution is skewed to the right and the median is the same. Still, this is an indication that the feedback system might help to reduce control effort by making it more clear for the driver what the vehicle is doing. This has the potential of increasing driving pleasure and comfort but more research is needed. The results of the evaluation form TLX do not show relevant differences in the different workload aspects between the situation with- and without additional

feedback. If the demand, effort and frustration are lumped together the combined p-value is 0.048 and the mean is 14 % lower with feedback. Drivers reported they liked their second run better in terms of comfort, safety, performance, pleasure and perceived grip level. Six drivers reported that the second run felt better, more natural, more intuitive or more succesful but they reported this was more due to familiarity with the vehicle and the road surface rather than the change in haptic feedback. Two drivers reported a shift in vehicle balance between over- and understeer which is in line with the differences found in vehicle states.

A comparison can be made between the results found in this load measurement based study and the results found in the model based HSNL study [4]. In the HSNL study no statistically significant differences were found for vehicle states during real car testing. The simulator tests showed reduced lateral error and SRR but real car testing did not confirm this. However, by using a measurement based approach in this thesis the haptic feedback is improved and differences are found for several vehicle states described above. The HSNL study did find statistically significant differences in the NASA TLX but the results found in this thesis do not confirm this result except when combining the different aspects of workload. Reason for this can be the limited size of the test group and limited time for each test subject in this thesis compared to the HSNL study. A recommendation for future work is to repeat the experiment with more test subjects and more time for each test subject. The disadvantage is that this costs more time and money and it might be more difficult to keep constant conditions.



---

# Discussion

## Load sensing bearings

With LSB measurements it is possible to reconstruct the lateral force and aligning moment of the tire in controlled conditions. Identification of the lateral force had been done before [13] and this thesis shows that identification of the aligning moment is also possible. However, the estimate of the aligning moment is not as good as the estimate of the lateral force. Both models are disturbed not only by random noise but also by forces- and moments acting on the tire in other directions. In close to steady-state cornering conditions with small longitudinal forces the Variance Accounted For (VAF) values for the lateral force are 95 to 100 percent whereas the values for the aligning moment are around 85 to 95 percent. The Multiple Linear Regression Analysis (MLRA) used to reconstruct the lateral force and aligning moment yields simple first order linear models. The first singular value is more than one order higher in magnitude which indicates that a first order model is capable of describing the main dynamics. The models can be improved by choosing a higher order and by using a more complex nonlinear approximation. However, other problems need a solution more urgent.

The first area of improvement is the bearing design and placement of the strain gauges and hall effect sensors. For the LSB design for the Opel Astra SKF had to modify the existing bearings and decided to mount three strain gauges between the three attachment points to the knuckle. However, from a load sensing point of view it would be better to take the placing of the strain gauges into account in the mechanical design of the bearing. Multiple strain gauges can then be mounted to different flexible parts of the bearing which are only deformed by a force in one direction. This can lead to a complete decoupling of the forces- and moments acting on the bearing and is similar to the concept of the VEHICLE LOAD SENSOR (VELOS) measurement wheel. The signal-to-noise ratio can be improved by a better design of the LSB such that passing of the balls in the bearing does not influence the measured deformations of the different flexible elements. This makes the filtering procedure less computationally demanding and more suitable for use in passenger vehicles. The disadvantage is that the mechanical design will be more complex, the cost will be higher and it can not be seen as an add-on for existing vehicles anymore.

Unfortunately the model of the lateral force in this thesis is mainly based on a shift in load transfer and a change in vertical force as the vehicle drives through the corner. The strain gauge model is based only on strain gauge measurements and the direction of the force can be identified without the use of the hall effect sensors because the load transfer is in different direction between a right- and a left hand corner. This means that the measurement will be completely different if the vehicle is for example driving over a bump. The measurements are also influenced by changes in longitudinal force. For straight line driving the lateral force estimate is useless because it is influenced by the longitudinal force which is much larger in amplitude than the lateral force. The bearings and models used in this thesis do not apply to more dynamic driving conditions and have to be improved as stated before.

Another problem that needs to be solved is the influence of temperature and bearing degradation on the measurements. If the temperature changes the measured strains will get an offset and therefor the reconstructed force- or moment will also get an offset. Difficulty here is that the temperature distribution over the bearing does not have to be uniform [19][20]. The bearing also slowly degrades over time which can cause an offset and introduce the need for recalibration. This influence needs to be investigated if the bearings need to last several decades in a vehicle. For this thesis the experiments are short to minimize the influence of temperature and drift and the reconstructed force- and aligning moment are zeroed every time the vehicle velocity is zero. A more permanent solution might be found by using temperature sensors and by revising the strain gauge layout to be able to use a full wheatstone bridge. It is also interesting to explore the possibilities to prevent drift with online recalibration using other sensors available in the vehicle.

The calibration procedure also needs to be improved to get better models. For real vehicle tests it is difficult to keep certain driver inputs or vehicle states at a constant level and also the test track has limitations. The results in this thesis are dependent on the datasets that are used for identification of the models. This is of course not desired and if the LSBs are taken into production it is not desired having to calibrate each bearing in a real vehicle test. The work done in [14] shows that BEaring Test SYstem (BETSY) can provide a feasible solution to calibrate the bearings but more research is needed to be able to obtain an accurate calibration which can be reproduced. Another option might be the use of tire testing facilities with a rolling road to simulate real driving and still have controlled conditions.

Previous studies [13] used strain gauges and eddy current sensors for identification of the forces and moments acting on the bearing. This thesis shows that Hall effect sensors can be a suitable alternative. Instead of directly measuring the deformation of the bearing housing with strain gauges, the hall effect sensors measure a tilting movement of the Anti-lock Braking System (ABS) ring. This might be really useful to measure the lateral force and aligning moment. Unfortunately the LSBs only have two hall effect sensors placed in a vertical line so it was only possible to identify a model to reconstruct the lateral force. These results look promising, especially taking into account the filtering that was needed to remove the oscillations caused by the holes in the ABS ring. The measurements might be less influenced by noise and longitudinal force because the hall effect sensors are not measuring bearing deformation directly. A recommendation for future work is to investigate identification with more than two hall effect sensors looking at a solid ring instead of a ring with holes. Again it would be best to incorporate this in the initial mechanical design of the bearing.



## Haptic feedback

Haptic feedback on the steering wheel can help the driver to keep control of a vehicle and thereby increase safety. The system developed in this thesis amplifies the drop in aligning moment as a vehicle approaches the handling limits. The HSNL study [4] did the same with a model based approach using slip angle measurements in combination with a tire model. The innovation in this thesis is that instead of measuring the slip angle and using a tire model the haptic feedback is now based directly on measurements of the lateral force and aligning moment with LSBs.

The results show a statistically significant reduction in left front wheel lateral force, front axle slip angle and vehicle body slip angle. The variance in lateral force and aligning moment are also reduced. These are all indications that the system can help the driver to prevent inputs leading to understeer. However, the total number of loss of control incidents was the same and no relevant differences are found in the comparison of vehicle speed, lateral acceleration, yaw-rate and cornering radius with- and without feedback. The goal of the system is to inform the driver about the available grip level such that the driver keeps control of the vehicle and prevents the tires from saturating. The result in this thesis shows that drivers are indeed more capable of preventing saturation of the front tires. However, the cornering radius is not found to be lower. It is interesting to see this result because the HSNL study [4] actually shows a statistically significant reduction in cornering radius. For the experiment it was possible to simply drive a larger radius and this could sometimes be beneficial because the available grip was a bit higher on the outside of the circle. But on a normal road increasing the radius will most likely mean driving off the road resulting in a crash. The presumption is still that drivers will in this case take it more slowly instead of increasing the radius but further investigation is needed for example by repeating the experiment with cones marking the outer radius of the road.

The SRR is lower with additional haptic feedback indicating a reduction in control effort for the driver. The driver is provided with more information about the available grip level and therefore it is easier to keep the vehicle in a steady-state condition close to the limit. However, the distribution is not normal and skewed to the right and hence the result is not very robust. The results of the evaluation form are not statistically significant but when different aspects of workload are combined this shows a reduction in workload with feedback. The test subjects liked their second run better but they reported this was more due to familiarity with the vehicle, road surface and the maneuver. For future experiments it is recommended to have more runs for each test subject to minimize the learning effect. Disadvantage is that this increases the cost and time needed for the experiment. It would be wise to start with simulator testing before actually testing in a real vehicle test such that the time and costs for real vehicle tests can be reduced. Two out of thirteen drivers reported a switch from understeer to oversteer behaviour with haptic feedback. This might be explained by the fact that the system used for the experiments is only based on load measurements of the front tires. Drivers can prevent saturation of the front tire lateral force but this is more difficult for the rear since there is no warning on the steering wheel if the rear tires lose grip. It is recommended to repeat the experiments with LSBs at the rear so the haptic feedback can also warn drivers before an oversteer situation.

By measuring the lateral force and the aligning moment of the tires it is not needed to measure the body slip angle of the vehicle to provide the haptic feedback. However, the algorithm creating the haptic feedback signal from measurements with the LSBs used in this thesis is very simple and only suitable to show the working principle of the haptic feedback. For use in passenger vehicles the algorithm should be completely revised. The first improvement can be reached by improving the measurements with the LSBs to obtain better estimates of the lateral force and aligning moment. Then still it is not desired to base the feedback directly on the tire road measurements and it is better to combine the measurements with a model for example using a kalman filter. Next to that the system should be adapted to work in more dynamic driving conditions. The effect of longitudinal and vertical force should also be taken into account because they both influence the way the tire contact patch deforms and thereby influence the pneumatic trail which defines the haptic feedback normally available to drivers. The influence of different parameters in front view such as the camber angle and the front view kingpin offset and kingpin inclination angle defining the scrub radius should be taken into account. The system also has to be adapted to work on different road surfaces. It is interesting to see how the measurements of the aligning moment and improvement in haptic feedback can be extended to other driving conditions for example to improve straight line stability.

Another important question is if the drop in aligning moment is really the best type of feedback for drivers. This type of feedback provides the driver with information about the available grip level but a different approach can be found in guiding the driver to the desired inputs [23]. The development of haptic guidance systems for example for obstacle avoidance or lane keeping purposes could also be extended to a vehicle driving on the limit in a corner. The author of this thesis tested this shortly but did not like the system because it felt like a restriction in steering wheel angle. However, further investigation is recommended to show the benefits of either approach and maybe how to combine them depending on different driving situations. For the tests on the particular surface with the Opel Astra the skidding of the tires generates vibrations in the steering wheel which is used by the drivers to feel that they are on the limit. This diminishes the effect of the additional haptic feedback system because the test subjects tend to use the vibrations next to the drop in aligning moment. However, this might also be a type of feedback which can be interesting for further investigation.

For future experiments with haptic feedback it is recommended to build the platform on a new vehicle which replaces the Opel Astra. If a new vehicle is used for haptic steering feedback a Rear-Wheel Drive (RWD) vehicle is recommended such that the front tires which determine the steering feel are not driven by the engine. Also the steering torque sensor needs to be improved. The sensor is self designed using strain gauges and the disadvantage is that it is influenced by forces in other directions than the wheel rotational direction and by vibrations of the steering wheel column caused by skidding of the tires. An ideal configuration would be using a full Electric Power Assisted Steering (EPAS) system including a steering torque sensor such that the desired haptic feedback can be added on top of a zero resistance basis. The measurements with the Opel Astra are also disturbed by fluctuations in the power supply. Possible explanation is the increase in current draw by the addition of the LSBs and Global Positioning System (GPS).

---

# Conclusion

## Load sensing bearings

Identification of the lateral force and aligning moment of the tires in steady-state cornering conditions is possible with LSBs but the measurements need to be improved.

- For optimal measurements and high signal-to-noise ratio the concept of load sensing should be incorporated in the mechanical design of the bearing and the placement of the sensors on the bearing housing may be further improved.
- An extensive filtering procedure is needed to remove noise caused by the multiples of the wheel rotational frequency and the ball pass frequency in the bearing.
- The estimates for steady-state cornering conditions are good but improvement is needed to account for the influence of other forces and moments in more dynamic driving situations and driving on a banked road and over bumps.
- The influence of temperature and drift due to bearing degradation over a longer period of time needs to be investigated and removed before adoption in passenger vehicles.
- The calibration procedure on a machine should be improved such that calibration on the real vehicle is not needed anymore. This enables better control of the inputs such that the calibration procedure can be repeated producing the same results.
- A first order linear model found by a MLRA can describe the main dynamics but higher order nonlinear models might be able to improve the estimates.
- With the current bearing design using three strain gauges and a linear model it is not possible to identify completely decoupled forces- and moments such as the VELOS measurement wheel is able to do.
- Hall effect sensors can be a good alternative for strain gauges but further experiments are needed with more hall effect sensors and a solid ring.

## Haptic feedback

Amplifying the drop in aligning moment as haptic feedback on the steering wheel can help the driver to prevent saturation of the lateral force of the front tires but more research is needed to investigate if this really increases safety, driving pleasure and comfort.

- The results show a statistically significant decrease in front wheel lateral force and front axle slip angle but for the particular experiment this does not show a statistically significant decrease in cornering radius. It is recommended to further investigate how the system can help to improve safety.
- The steering wheel reversal rate and combined workload aspects on the evaluation form show a decrease with haptic feedback indicating a decrease in control effort for the driver with haptic feedback.
- The measurements with LSBs should be improved if they are used for the haptic feedback in more dynamic driving conditions on a normal road. The system should be extended with measurements from LSBs in the rear wheels such that the system can also warn the driver in case the rear tires are closer to the limit.
- The haptic feedback algorithm has to be extended taking longitudinal and vertical force into account for more dynamic driving conditions and the system should be adapted to work on different road surfaces. A more sophisticated system does not use the load measurements directly but rather uses a method combining the measurements with a model for example using a kalman filter.
- Load sensing can be used for different kinds of haptic feedback and it is interesting to explore the possibilities in different driving conditions for different types of haptic feedback.
- It is recommended to perform the experiment with more drivers and more runs for each driver to minimize the learning effect and find more statistically significant results. To save cost and time the real vehicle test could be preceded by simulator experiments.
- For future experiments with haptic feedback it is recommended to revise the instrumentation and build it on a different platform than the Opel Astra. A different way of measuring steering torque is needed and the problems with fluctuations in the power supply need to be solved.
- A different car on a different road surface can help to minimize the steering column vibrations due to tire skidding which diminishes the haptic feedback effect caused by the drop in aligning moment.
- If wheel load measurements are available in a vehicle the haptic feedback system could simply be a piece of software making the EPAS system more dynamic without the need for additional hardware.


---

## Appendix A

---

# **Bearing information**



Edition /Year Month		1 / 0208	2 /	3 /	4 /	5 /	6 /		
SKF				Drawn	Checked	Approved	R.C. 29	T.C.	©
				B.C.	A.S.	D.B.	Dat. 23-08-2002		
	HUB UNIT 3E ( OPEL )			Product Designation					
				BAR-0050 AB					
				CAD model no. RX0010882					

**Figure A-2:** Bearing cross section drawing specifications

Pitch circle dia.            62  
 Size of balls                 11.112  
 N. of balls                    2 x 16  
 Contact angle                36°

Bearing preloaded

Grease type                  GHG  
 Filling grade                40 – 50 % of void (6 – 7.5 g.)

Environmental protection to QU 000 001  
 ----- Hardened surfaces with induction heating

**Figure A-3:** Opel Astra front wheel bearing detailed information





---

## Appendix B

---

# Wheatstone bridge

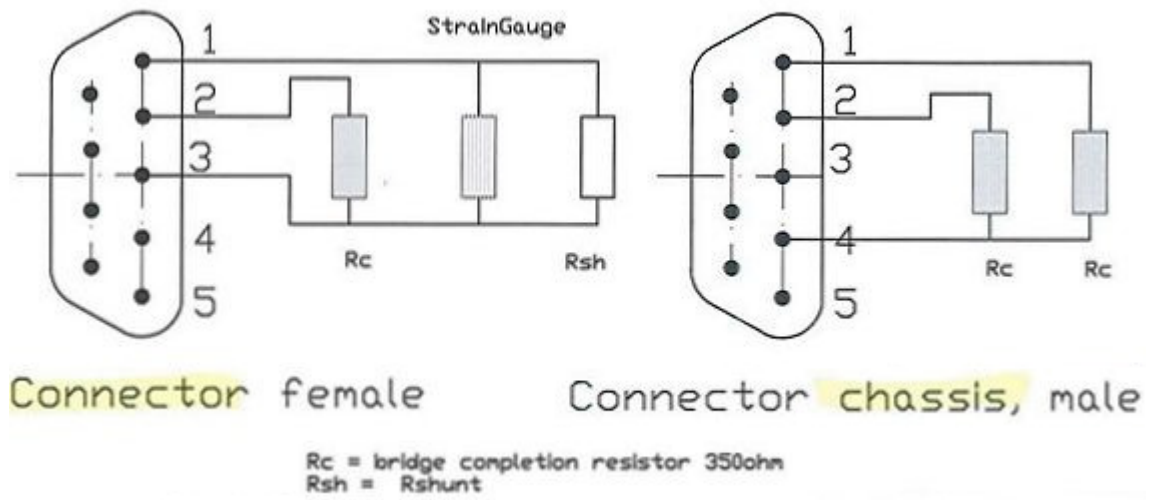


Figure B-1: Precision resistors in the connectors on the strain gauge conditioner

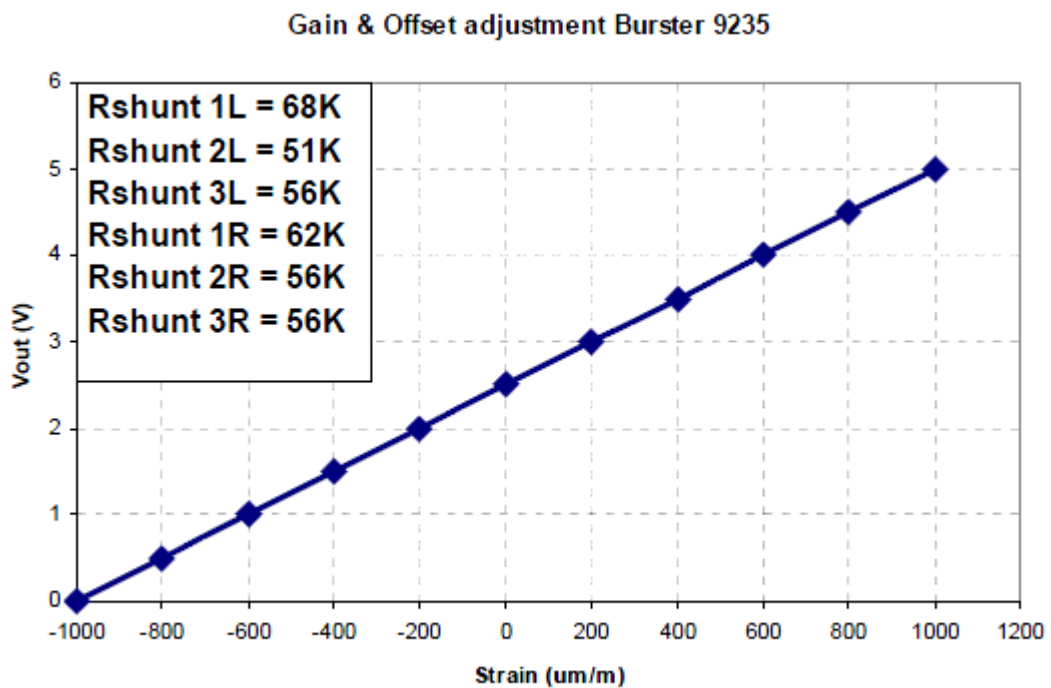


Figure B-2: Shunt values wheatstone bridge completion six strain gauges

---

## Appendix C

---

### **Simulink model haptic controller**

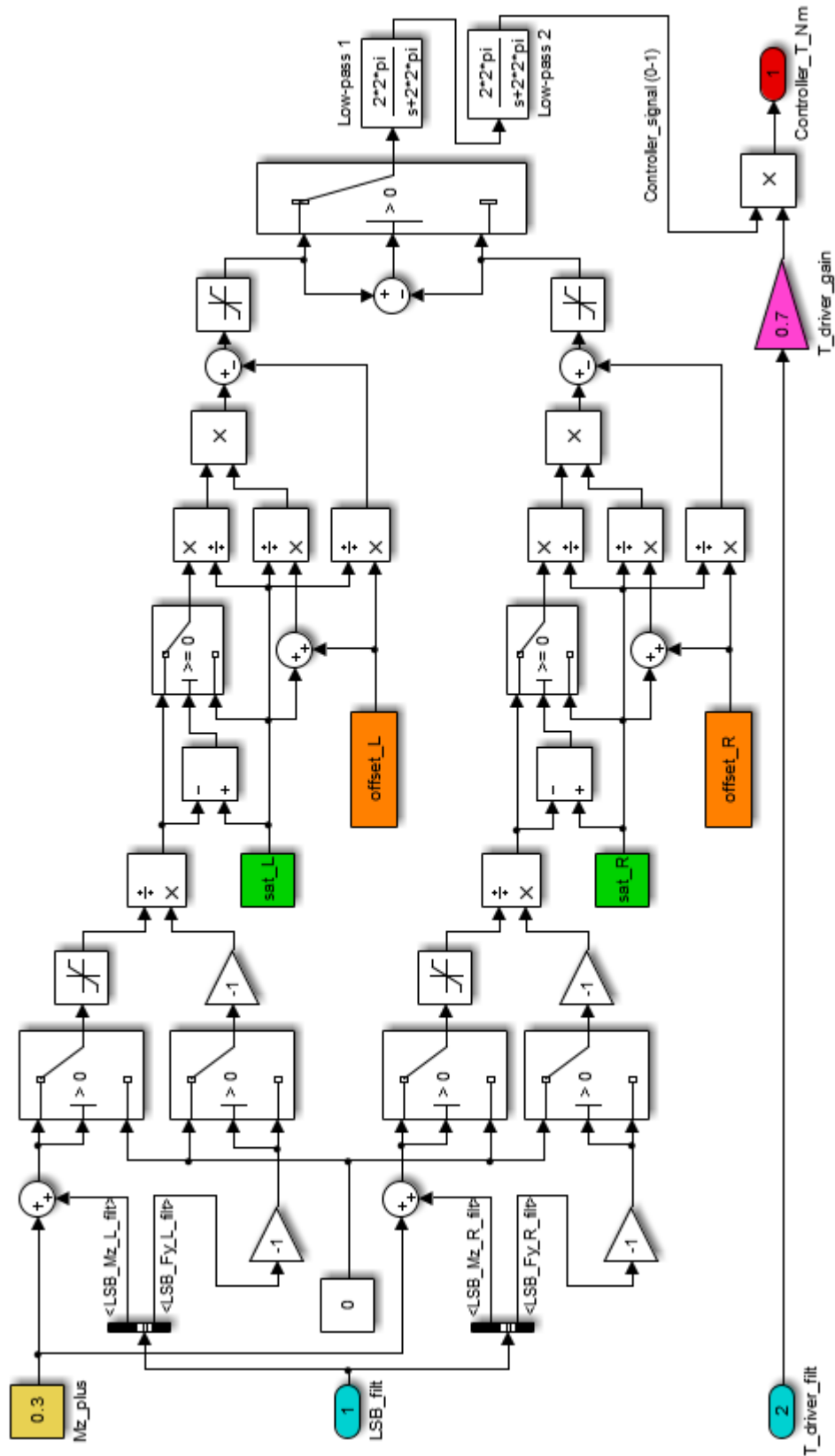


Figure C-1: Simulink model of the used haptic feedback controller

---

## Appendix D

---

### **Evaluation form**

*Answers are confidential: none of this information will be published related to your name.  
Feel free to leave out any details you feel uncomfortable to fill in.*

### Personal details

Name: \_\_\_\_\_

Male | Female

Age: \_\_\_\_\_

### Driving experience

Professional driving experience?

Number of years owning driving license:

Number of cars owned:

Number of crashes involved (on public road):

How would you grade your driving skills:

BAD

1 | 2 | 3 | 4 | 5 | 6 | 7 | 8 | 9 | 10

GOOD

*Please read the questions and scale below carefully and tick the correct box.*

MENTAL DEMAND: HOW MENTALLY DEMANDING WAS THE TASK?																			
VERY LOW	<input type="checkbox"/>	<input type="checkbox"/>	<input type="checkbox"/>	<input type="checkbox"/>	<input type="checkbox"/>	<input type="checkbox"/>	<input type="checkbox"/>	<input type="checkbox"/>	<input type="checkbox"/>	<input type="checkbox"/>	<input type="checkbox"/>	<input type="checkbox"/>	<input type="checkbox"/>	<input type="checkbox"/>	<input type="checkbox"/>	<input type="checkbox"/>	<input type="checkbox"/>	<input type="checkbox"/>	VERY HIGH
PHYSICAL DEMAND: HOW PHYSICALLY DEMANDING WAS THE TASK?																			
VERY LOW	<input type="checkbox"/>	<input type="checkbox"/>	<input type="checkbox"/>	<input type="checkbox"/>	<input type="checkbox"/>	<input type="checkbox"/>	<input type="checkbox"/>	<input type="checkbox"/>	<input type="checkbox"/>	<input type="checkbox"/>	<input type="checkbox"/>	<input type="checkbox"/>	<input type="checkbox"/>	<input type="checkbox"/>	<input type="checkbox"/>	<input type="checkbox"/>	<input type="checkbox"/>	<input type="checkbox"/>	VERY HIGH
TEMPORAL DEMAND: HOW HURRIED OR RUSHED WAS THE PACE OF THE TASK?																			
VERY LOW	<input type="checkbox"/>	<input type="checkbox"/>	<input type="checkbox"/>	<input type="checkbox"/>	<input type="checkbox"/>	<input type="checkbox"/>	<input type="checkbox"/>	<input type="checkbox"/>	<input type="checkbox"/>	<input type="checkbox"/>	<input type="checkbox"/>	<input type="checkbox"/>	<input type="checkbox"/>	<input type="checkbox"/>	<input type="checkbox"/>	<input type="checkbox"/>	<input type="checkbox"/>	<input type="checkbox"/>	VERY HIGH
PERFORMANCE: HOW SUCCESSFUL WERE YOU IN ACCOMPLISHING WHAT YOU WERE ASKED TO DO?																			
PERFECT	<input type="checkbox"/>	<input type="checkbox"/>	<input type="checkbox"/>	<input type="checkbox"/>	<input type="checkbox"/>	<input type="checkbox"/>	<input type="checkbox"/>	<input type="checkbox"/>	<input type="checkbox"/>	<input type="checkbox"/>	<input type="checkbox"/>	<input type="checkbox"/>	<input type="checkbox"/>	<input type="checkbox"/>	<input type="checkbox"/>	<input type="checkbox"/>	<input type="checkbox"/>	<input type="checkbox"/>	FAILURE
EFFORT: HOW HARD DID YOU HAVE TO WORK TO ACCOMPLISH YOUR LEVEL OF PERFORMANCE?																			
VERY LOW	<input type="checkbox"/>	<input type="checkbox"/>	<input type="checkbox"/>	<input type="checkbox"/>	<input type="checkbox"/>	<input type="checkbox"/>	<input type="checkbox"/>	<input type="checkbox"/>	<input type="checkbox"/>	<input type="checkbox"/>	<input type="checkbox"/>	<input type="checkbox"/>	<input type="checkbox"/>	<input type="checkbox"/>	<input type="checkbox"/>	<input type="checkbox"/>	<input type="checkbox"/>	<input type="checkbox"/>	VERY HIGH
FRUSTRATION: HOW INSECURE, DISCOURAGED, IRRITATED, STRESSED AND ANNOYED WERE YOU?																			
VERY LOW	<input type="checkbox"/>	<input type="checkbox"/>	<input type="checkbox"/>	<input type="checkbox"/>	<input type="checkbox"/>	<input type="checkbox"/>	<input type="checkbox"/>	<input type="checkbox"/>	<input type="checkbox"/>	<input type="checkbox"/>	<input type="checkbox"/>	<input type="checkbox"/>	<input type="checkbox"/>	<input type="checkbox"/>	<input type="checkbox"/>	<input type="checkbox"/>	<input type="checkbox"/>	<input type="checkbox"/>	VERY HIGH

**Figure D-1:** Front side of evaluation form used for final test

**FILL IN THIS PAGE AFTER DRIVING THE SECOND RUN!!!**

MENTAL DEMAND: HOW MENTALLY DEMANDING WAS THE TASK?																			
VERY LOW	<input type="checkbox"/>	<input type="checkbox"/>	<input type="checkbox"/>	<input type="checkbox"/>	<input type="checkbox"/>	<input type="checkbox"/>	<input type="checkbox"/>	<input type="checkbox"/>	<input type="checkbox"/>	<input type="checkbox"/>	<input type="checkbox"/>	<input type="checkbox"/>	<input type="checkbox"/>	<input type="checkbox"/>	<input type="checkbox"/>	<input type="checkbox"/>	<input type="checkbox"/>	<input type="checkbox"/>	VERY HIGH
PHYSICAL DEMAND: HOW PHYSICALLY DEMANDING WAS THE TASK?																			
VERY LOW	<input type="checkbox"/>	<input type="checkbox"/>	<input type="checkbox"/>	<input type="checkbox"/>	<input type="checkbox"/>	<input type="checkbox"/>	<input type="checkbox"/>	<input type="checkbox"/>	<input type="checkbox"/>	<input type="checkbox"/>	<input type="checkbox"/>	<input type="checkbox"/>	<input type="checkbox"/>	<input type="checkbox"/>	<input type="checkbox"/>	<input type="checkbox"/>	<input type="checkbox"/>	<input type="checkbox"/>	VERY HIGH
TEMPORAL DEMAND: HOW HURRIED OR RUSHED WAS THE PACE OF THE TASK?																			
VERY LOW	<input type="checkbox"/>	<input type="checkbox"/>	<input type="checkbox"/>	<input type="checkbox"/>	<input type="checkbox"/>	<input type="checkbox"/>	<input type="checkbox"/>	<input type="checkbox"/>	<input type="checkbox"/>	<input type="checkbox"/>	<input type="checkbox"/>	<input type="checkbox"/>	<input type="checkbox"/>	<input type="checkbox"/>	<input type="checkbox"/>	<input type="checkbox"/>	<input type="checkbox"/>	<input type="checkbox"/>	VERY HIGH
PERFORMANCE: HOW SUCCESSFUL WERE YOU IN ACCOMPLISHING WHAT YOU WERE ASKED TO DO?																			
PERFECT	<input type="checkbox"/>	<input type="checkbox"/>	<input type="checkbox"/>	<input type="checkbox"/>	<input type="checkbox"/>	<input type="checkbox"/>	<input type="checkbox"/>	<input type="checkbox"/>	<input type="checkbox"/>	<input type="checkbox"/>	<input type="checkbox"/>	<input type="checkbox"/>	<input type="checkbox"/>	<input type="checkbox"/>	<input type="checkbox"/>	<input type="checkbox"/>	<input type="checkbox"/>	<input type="checkbox"/>	FAILURE
EFFORT: HOW HARD DID YOU HAVE TO WORK TO ACCOMPLISH YOUR LEVEL OF PERFORMANCE?																			
VERY LOW	<input type="checkbox"/>	<input type="checkbox"/>	<input type="checkbox"/>	<input type="checkbox"/>	<input type="checkbox"/>	<input type="checkbox"/>	<input type="checkbox"/>	<input type="checkbox"/>	<input type="checkbox"/>	<input type="checkbox"/>	<input type="checkbox"/>	<input type="checkbox"/>	<input type="checkbox"/>	<input type="checkbox"/>	<input type="checkbox"/>	<input type="checkbox"/>	<input type="checkbox"/>	<input type="checkbox"/>	VERY HIGH
FRUSTRATION: HOW INSECURE, DISCOURAGED, IRRITATED, STRESSED AND ANNOYED WERE YOU?																			
VERY LOW	<input type="checkbox"/>	<input type="checkbox"/>	<input type="checkbox"/>	<input type="checkbox"/>	<input type="checkbox"/>	<input type="checkbox"/>	<input type="checkbox"/>	<input type="checkbox"/>	<input type="checkbox"/>	<input type="checkbox"/>	<input type="checkbox"/>	<input type="checkbox"/>	<input type="checkbox"/>	<input type="checkbox"/>	<input type="checkbox"/>	<input type="checkbox"/>	<input type="checkbox"/>	<input type="checkbox"/>	VERY HIGH

Did you notice a difference in steering behavior between the first and second run?

Yes | No

*For the next questions please encircle the correct word. If there was no difference please encircle both words.*

I drove the *first / second* run with additional feedback on the steering wheel

I felt more comfortable during the *first / second* run.

I felt safer during the *first / second* run.

I liked my performance during the *first / second* run better.

I had more pleasure during the *first / second* run.

I could feel the available grip level better during the *first / second* run.

**General comments**

---



---



---



---

Thank you for your participation!

**Figure D-2:** Back side of evaluation form used for final test





---

## Appendix E

---

# Vehicle parameters

**Table E-1:** Vehicle parameters Opel Astra [24] [4]

Parameter	Value
Weight	1155 kg
Wheelbase	2.61 m
Track width front	1.49 m
Track width rear	1.46 m
Weight distribution front	65 %
Tire size	195/60R15
Steering ratio	1:16.4
Driven wheels	Front 2
Gearbox	Manual 5
COG height	0.2 m

---

# Bibliography

- [1] S. M. Savaresi and M. Tanelli, *Active Braking Control Systems Design for Vehicles*. Advances in Industrial Control (AIC), 2007.
- [2] E. K. Liebemann, K. Meder, J. Schuh, and G. Nenninger, “Safety and Performance Enhancement: The Bosch Electronic Stability Control (ESP),” *SAE International*, October 2004.
- [3] National Highway Traffic System Administrator, “Electronic Stability Control System,” *FMVSS*, March 2007.
- [4] D. I. Katzourakis, *Driver Steering Support Interfaces Near the Vehicle’s Handling Limits*. PhD thesis, Delft University of Technology, 2012.
- [5] R. Parasuraman and V. Riley, “Human and Automation: Use, Misuse, Disuse, Abuse,” *Human Factors*, vol. 39, pp. 230–253, June 1997.
- [6] J. C. F. de Winter and D. Dodou, “Preparing drivers for dangerous situations: A critical reflection on continuous shared control,” *IEEE International Conference on Systems, Man, and Cybernetics (SMC)*, pp. 1050–1056, October 2011.
- [7] M. K. Hassan, N. A. M. Azubir, H. M. I. Nizam, S. F. Toha, and B. S. K. K. Ibrahim, “Optimal Design of Electric Power Assisted Steering System (EPAS) Using GA-PID Method,” *Procedia Engineering International Symposium on Robotics and Intelligent Sensors (IRIS)*, vol. 41, no. 3, pp. 614 – 621, 2012.
- [8] J. J. van Doornik, “Haptic feedback on the steering wheel near the vehicle’s handling limits using wheel load sensing,” Literature survey, Delft University of Technology, 2014.
- [9] J. S. Jermakian, “Crash avoidance potential of four passenger vehicle technologies,” *Accident Analysis and Prevention*, vol. 43, pp. 732 – 740, May 2011.
- [10] W. Dick, M. Lannoije, J. Schuller, and M. Reuter, “Dynamic Steering in the Audi Q5,” *ATZextra worldwide*, vol. 13, pp. 66 – 73, June 2008.

- [11] W. F. Milliken and D. L. Milliken, *Race car vehicle dynamics*. SAE International, 1995.
- [12] Y. H. J. Hsu and J. C. Gerdes, "Estimation of Tire Slip Angle and Friction Limits Using Steering Torque," *IEEE Transactions on Control Systems Technology*, vol. 18, pp. 896–907, July 2010.
- [13] J. A. den Engelse, "Estimation of the lateral force acting at the tire contact patch of a vehicle wheel using a hub bearing unit instrumented with strain gauges and Eddy-current sensors," Master's thesis, Delft University of Technology, 2013.
- [14] A. Jayashankar, "Experimental & Modeling Study of the Influence of Support Stiffness on Load Sensing Bearings," Master's thesis, Delft University of Technology, 2011.
- [15] D. C. Montgomery and E. A. Peck, *Introduction to Linear Regression Analysis*. John Wiley and Sons, 1992.
- [16] BS ISO 4138:2004, British Standard International Organization for Standardization, "2004",.
- [17] Kistler, "VELOS instruction manual."
- [18] M. Verhaegen and V. Verdult, *Filtering and System Identification: A Least Squares Approach*. Cambridge University Press, 2007.
- [19] D. T. J. de Bot, "The thermal model of a load sensing hub bearing unit," Literature survey, Delft University of Technology, 2009.
- [20] D. T. J. de Bot, "A temperature state estimator for a load sensing hub bearing unit," Master's thesis, Delft University of Technology, 2009.
- [21] Google, *Google Maps*. Google Inc., viewed 2014.
- [22] M. R. Savino, "Standardized Names and Definitions for Driving Performance Measures," Master's thesis, Tufts University, 2009.
- [23] M. Della Penna, M. M. van Paassen, D. A. Abbink, M. Mulder, and M. Mulder, "Reducing Steering Wheel Stiffness is Beneficial in Supporting Evasive Maneuvers," *IEEE International Conference on Systems, Man, and Cybernetics (SMC)*, pp. 1628–1635, October 2010.
- [24] J. van Gerwen, "Haptic feedback on the steering wheel to maximize front axle grip," Master's thesis, Delft University of Technology, 2012.

---

# Glossary

## List of Acronyms

<b>ABS</b>	Anti-lock Braking System
<b>ACC</b>	Adaptive Cruise Control
<b>ADAS</b>	Advanced Driver Assistance Systems
<b>AFS</b>	Active Front Steering
<b>APGS</b>	Advanced Parking Guidance System
<b>BETSY</b>	BEaring Test SYstem
<b>BLIS</b>	BLindspot Information System
<b>CAN</b>	Controller Area Network
<b>CE</b>	Control Engineering
<b>COG</b>	Center Of Gravity
<b>DC</b>	Direct Current
<b>EPAS</b>	Electric Power Assisted Steering
<b>ESC</b>	Electronic Stability Control
<b>ESP</b>	Electronic Stability Program
<b>FWD</b>	Front-Wheel Drive
<b>GPS</b>	Global Positioning System
<b>HPAS</b>	Hydraulic Power Assisted Steering
<b>HSNL</b>	Haptic Support Near the Limits
<b>IMU</b>	Inertial Measurement Unit

<b>IPAS</b>	Intelligent Parking Assist System
<b>ISO</b>	International Organization for Standardization
<b>LDW/P</b>	Lane Departure Warning / Prevention
<b>LSB</b>	Load Sensing Bearing
<b>MABX</b>	MicroAutoBoX
<b>ME</b>	Mechanical Engineering
<b>MLRA</b>	Multiple Linear Regression Analysis
<b>NASA</b>	National Aeronautics and Space Administration
<b>OCAS</b>	Obstacle Collision Avoidance System
<b>RMS</b>	Root Mean Square
<b>RWD</b>	Rear-Wheel Drive
<b>SRR</b>	Steering wheel Reversal Rate
<b>SVD</b>	Singular Value Decomposition
<b>SWIFT</b>	Spinning Wheel Integrated Force Transducer
<b>TJA</b>	Traffic Jam Assist(ant)
<b>TLX</b>	Task Load Index
<b>TU Delft</b>	Delft University of Technology
<b>VAF</b>	Variance Accounted For
<b>VELOS</b>	VEhicle LOad Sensor

## List of Symbols

$\alpha_f$	Front axle slip angle
$\alpha_r$	Rear axle slip angle
$\beta$	Vehicle slip angle
$\beta_0$	Vector with constant terms Multiple Linear Regression Analysis (MLRA)
$\beta_1$	Matrix with multiplication terms MLRA
$\epsilon$	Vector with strains
$\gamma$	Kingpin inclination angle
$\hat{y}$	Estimated output
$\lambda$	Longitudinal slip

---

$\mu$	Tire-road friction coefficient
$\nu$	Caster angle
$\omega$	Frequency
$\omega$	Wheel angular velocity
$\omega_f$	Variable frequency velocity dependent notch filter
$\omega_{ballpass}$	Ball pass frequency
$\sigma$	Matrix with singular values on the diagonal
$\theta$	Angle
$\theta_{dot,sw}$	Steering wheel angular velocity
$\theta_{sw}$	Steering wheel angle
$a_x$	Longitudinal acceleration
$a_y$	Lateral acceleration
$a_z$	Vertical acceleration
$C$	Normalized signal haptic feedback controller
$c$	Constant, see $Mz\_plus$
$D_{ir}$	Diameter bearing inner ring
$D_{or}$	Diameter bearing outer ring
$F_x$	Longitudinal force
$F_y$	Lateral force
$F_z$	Vertical force
$FM$	Vector with Forces and Moments
$g$	Gravitational acceleration, $9.81 \text{ m/s}^2$
$K_{mu}$	Gain
$M_x$	Overturning moment
$M_y$	Rolling resistance moment
$M_z$	Aligning moment / aligning torque
$Mz\_plus$	Tuning parameter haptic feedback, see $c$
$N$	Number of datapoints
$n$	Model order
$offset$	Tuning parameter haptic feedback
$p_m$	Mechanical trail
$p_t$	Pneumatic trail
$Q_{xx}$	Q-matrix QR-factorization
$r$	Tire radius
$r$	Yaw-rate
$r_{value}$	R-value notch filter
$R_{xx}$	R-matrix QR-factorization
$sat$	Tuning parameter haptic feedback
$T$	Torque
$T_d$	Driver steering torque

---

$T_m$	Motor torque
$T_s$	Sampling time
$U$	Unitary matrix left side Singular Value Decomposition (SVD)
$u$	Input
$U_{1,n,N}$	Hankel input matrix
$V$	Absolute velocity
$V$	Unitary matrix right side SVD
$V_x$	Longitudinal velocity
$V_y$	Lateral velocity
$VAF$	Variance Accounted For
$w_{ballcarrier}$	Ball carrier frequency
$y$	Measured output
$Y_{1,n,N}$	Hankel output matrix